DESIGN OF AN EXPERIMENTAL THRUST NOZZLE TEST STAND

By

GERALD R. SEEMANN

Bachelor of Science

Texas Technological College

Lubbock, Texas

1959

Submitted to the faculty of the Graduate School of
the Oklahoma State University
in partial fulfillment of the requirements
for the degree of
MASTER OF SCIENCE
August, 1960

DESIGN OF AN EXPERIMENTAL THRUST

NOZZLE TEST STAND

Thesis Approved:

Glen W. Zumwalt
Thesis Adviser

J H Boggs

Robert MacVicar
Dean of the Graduate School

ACKNOWLEDGEMENT

The writer wishes first to express his appreciation to Professor J. H. Boggs and the Mechanical Engineering School for the financial assistance which made possible this year of study.

Indebtedness to Dr. Glen W. Zumwalt, Assistant Professor of Mechanical Engineering, for his guidance, time, and constructive criticism is acknowledged. These were invaluable and greatly appreciated.

Helpful suggestions and assistance of Assistant Professor Bert S. Davenport, the competent help of laboratory technicians, George Cooper and J. A. McCandless, and the efforts of Mr. Harris and the Research Apparatus Development Laboratory were of considerable aid.

The writer wisher also to thank Mrs. Mildred Avery and Miss Randye Grinstead for their help in typing the manuscript.

TABLE OF CONTENTS

LIST OF TABLES

LIST OF PLATES

LIST OF FIGURES

LIST OF FIGURES (Continued)

CHAPTER I

INTRODUCTION

The recent development of jet propulsion and rocket motors has re-aroused interest in the thrust or reaction force produced by a gas jet. Some forty to fifty years ago there was a similar interest during the development of steam turbines. This interest has grown out of practical problems associated with the operation of aircraft and missiles at supersonic speeds and higher altitudes. High speed flight necessitates specially designed engine components. It is extremely important that the jet nozzle of a rocket installation operating at these high speeds should have high internal efficiency, because a small loss in jet thrust results in a large loss in net thrust.

The testing of rockets, as opposed to reciprocating engines, presents to the experimenter the problem of measuring forces rather than shaft power. The measurement of the thrust force may be accomplished by direct methods in which the force is transmitted to an instrument designed to respond to this specific stimulus; or it may be done by indirect procedure involving measurement of one or more properties of the system which can be related to the thrust. This writing is concerned only with laboratory apparatus and not with the full scale testing of "hot" rocket motors which has been dealt with by Bierlein and Scheller (20)*; also consideration will be given only to the direct thrust measurement. In laboratory simulation of thrust nozzles, the gas supply pipe creates a major problem, since its rigidity must be accounted for in measuring thrust.

Many laboratory thrust nozzle test stands have been built by different investigators. The designs are numerous and various, depending upon the method of measurement selected. In view of the growing interest, and as part of a project to develop the gas dynamics experimental facilities at Oklahoma State University, there arose a need for designing a thrust nozzle test stand. This design is the principal concern of this thesis.

The purpose of the study contained in this thesis was twofold. The first aim was to design a thrust nozzle test stand flexible enough to permit adjustment for various experimental research while incorporating the best features possible for accuracy of direct thrust measurement. The second aim was to design a non-pumping ejector system to lower the back pressure, enabling a more realistic rocket nozzle performance to be realized from the experimental work.

* Numbers in parentheses refer to references in the bibliography.

CHAPTER II

PREVIOUS INVESTIGATIONS

In the past, the laboratory thrust nozzle test stand has proved to be a very valuable tool for exploring nozzle performance. The use of the test stand has become an invaluable aid to research projects connected with the probing of outer space. Some of the early developments of the direct thrust measuring devices, followed by descriptions of more recent laboratory test stands, are presented in this chapter in order that basic design considerations may be compared with the apparatus described in this thesis.

Four commonly used methods of measuring thrust directly are:

a) Flexure -- the jet reaction is arranged to bend the supply pipe, which is relatively stiff.

b) Free Movement -- the nozzle is free to move under its own reaction but restrained by a measuring device.

c) Free Movement With Soft Flexure -- this is a combination of the two previous methods but the resistance of the supply line is very small compared with the reaction force.

d) Thrust Comparison -- this measures the difference between the thrusts of opposing nozzles. The measurement may be any one of the previous methods.

One of the earliest attempts to measure nozzle thrust reaction used the flexure method. (Type a). This is the most simple method mechanically. The supply pipe may be supported as a cantilever with the nozzle arranged to discharge perpendicularly from its free end. The thrust may be measured by recording the deflection, by measuring strain in the pipe, or by supporting the free end on a weighing scale and discharging upwards. The main disadvantage of the method is that the stiffness of the pipe varies with the internal pressure and with temperature changes, especially local ones at the encastered end. Reproducible results require elaborate precaution to avoid these difficulties and even then accuracies are not likely to be better than ±1%.

Resenhain in 1900 (1) used the flexure method with the nozzle mounted to discharge horizontally from the bottom of a vertical supply pipe the upper end of which was rigidly supported. The null displacement method of force measurement was used by applying weights to compensate for the nozzle reaction. (Figure 1). The nozzles used were of the order of 0.18" throat diameter and steam was supplied at between twenty and two hundred psi. The thrust reaction varied be- between about one and eight pounds. The prime object of the investigation was to verify that obstructions in the jet did not affect the thrust. It is claimed that the steam pressure was measured to ±1.0 psi. In view of the method of weighing used and the effect of temperature on the flexibility of the vertical pipe it is unlikely that the thrust was measured with greater precision than ±0.1 pounds which is some 1% of the maximum recorded and 10% of the minimum.

Fletcher (1953) and Ashwood (1957) (2) balanced the flexure of

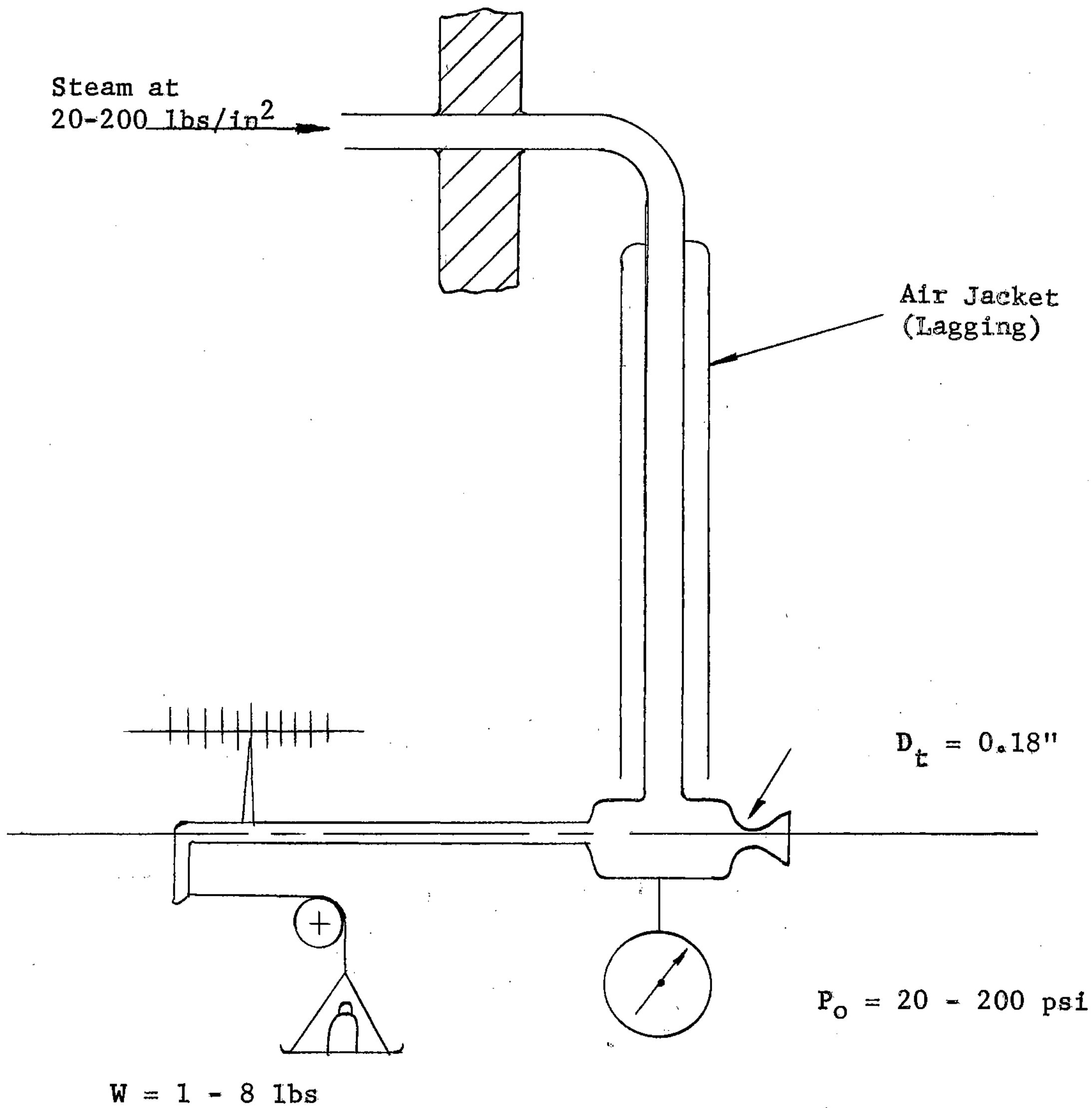

Fig. 1. Rosenhain (1900) Thrust Stand

a horizontal feed pipe to measure the reaction of an air jet. (Figure 2). The reaction was measured by strain gages at the root of the feed pipe. The cantilever pipe was 80 inches long and of 3-inch bore with 1/9-inch wall thickness. A strain measuring section was machined at the encastered end and top and bottom strain gauges were cemented to the surface, thoroughly dried, and then sealed in perspex boxes. Calibration was obtained by suspending weights on the line of action of the thrust. The nozzles were 1-inch throat diameter and air was supplied at up to 150 psi reservoir pressure. The maximum thrust was about 150 pounds. The sensitivity of this instrument was ± 0.2 pounds, but the overall accuracy based on repeated tests was more like ± 1.5 pounds. The strain gauges were very sensitive to local changes in temperature and this proved troublesome. It was necessary to run the apparatus for about twenty minutes to establish thermal equilibrium before taking a reading. Although reasonably accurate when used with care, this apparatus was eventually abandoned in favor of a system of free movement.

The free movement method of measurement (Type b) is perhaps the most popular today. (3). One method of allowing free movement is to support the entire reservoir of gas together with the nozzle and connections. It is the usual way of testing solid fuel rocket motors. However, when air or other cold gases are used, the weight of the reservoir to be supported is large compared with the thrust that can be maintained for a useful operating time. The alternative to supporting the entire apparatus is to provide some type of joint which will

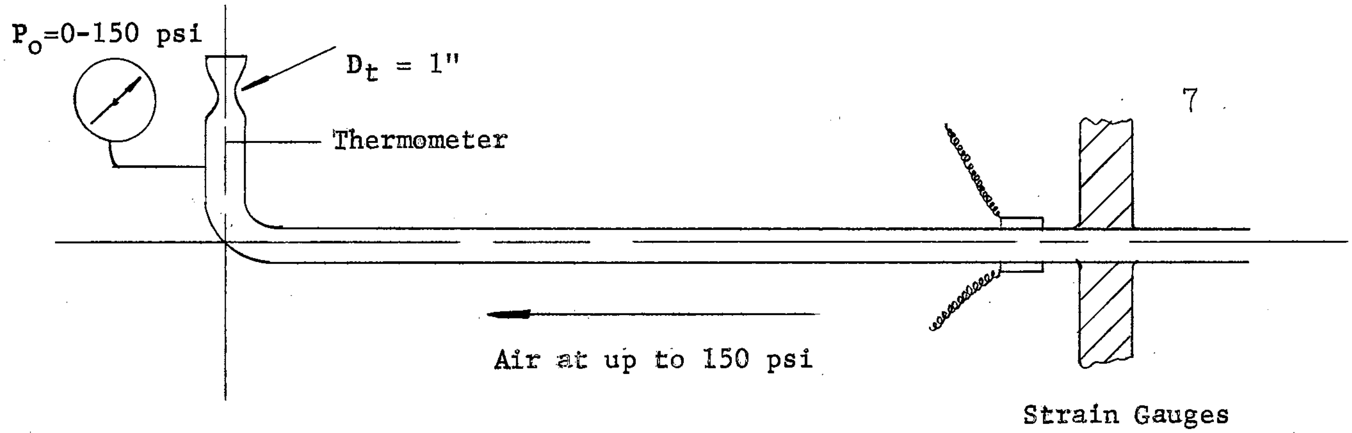

Fig. 2. Fletcher (1953) and Ashwood (1957) Apparatus

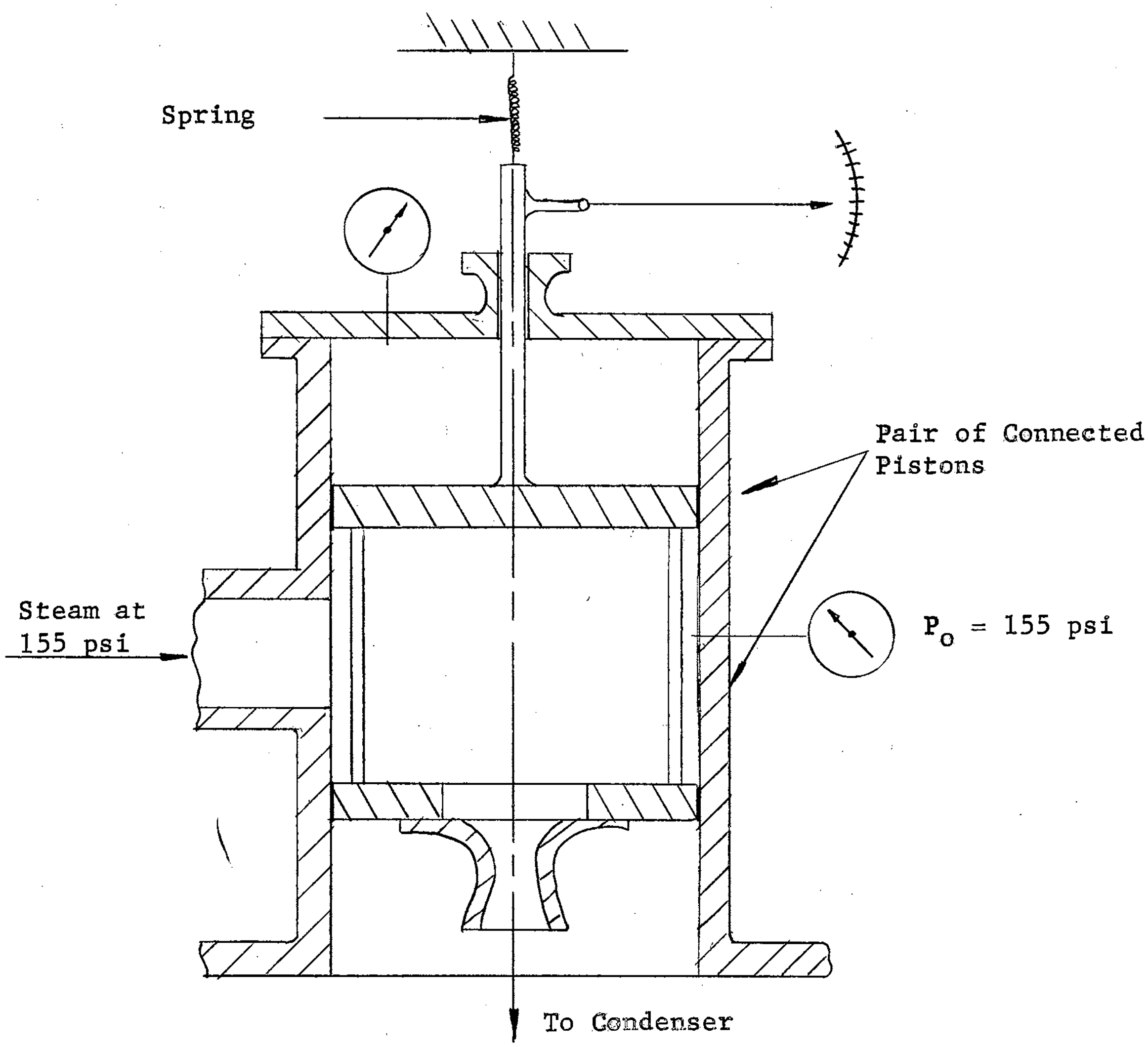

Fig. 3. Sibley and Kemble (1909) Thrust Stand

allow the nozzle to move freely through a limited distance. The difficulty with such joints is that they leak excessively when free or else are too stiff when virtually sealed. Often a small leak can be tolerated. Two forms that have been commonly used are a piston in which axial movements occur and a rotary joint. The piston is more prone to the characteristic faults of this method, but it occupies far less space. With the use of labyrinth glands, rotary joints can be made virtually leak proof, yet almost frictionless. Long leverage can be used to reduce the friction to a very small proportion of the measured thrust. With rotary joints, at least one elbow is needed in the supply pipe and the gas may pass a number of bends before reaching the nozzle. The assembly may be quite a large structure. Free movement, particularly with rotary joints, can lead to thrust apparatus of high precision. Several workers have noted sensitivities of the order of $\pm 0.1\%$. (3).

Sibley and Kemble (1909) (4) used an ingenious design in a thrust rig allowing free movement. (Figure 3). Steam was admitted through the wall of a cylinder at a point between two pistons. The pistons were linked together and the lower one had a center orifice to which the test nozzles were attached. The top piston was suspended from a coil spring and a rod which passed through a gland at the top of the cylinder. The lower end of the cylinder was connected to a condenser. The thrust was measured by the movement of the piston assembly. This apparatus was not a success, for, if the pistons were free when cold, they would bind when hot. When they were made sufficiently undersize to be free when hot, there was excessive steam leakage and condensation at the top of the piston. The apparatus was eventually abandoned in favor of a vertical flexure pipe. It would probably have been suitable with air at room temperature.

Fraser, Connor, and Coulter (1946) (5), Fraser and Rowe (1954) (3), and Fraser, Rowe, and Coulter (1957) (3) have used a particularly compact reaction apparatus that allows the nozzle free movement. (Figure 4). The movable member A is a hollow piston which acts as part of the main supply pipe and carries the nozzle B. The piston is a close sliding fit on three diameters, the upper and lower diameters being equal and the middle one being $\sqrt{2}$ times the smaller ones. The static pressure in the supply pipe acts upward on the smaller area of the movable member A and, through drillings provided in the wall, downward on the annular area at C. Since these areas are made equal, the resultant thrust due to static pressure is zero. The nozzle reaction acts downward and is received by oil in the other annulus D. In order to minimize friction, no pressure seals are employed on the movable member. Instead, small clearances and long leakage paths are relied upon to ensure that the rate of leakage of air is small compared with the discharge through the nozzle. The quantity of oil which leaks past the piston is very small compared with the swept volume of the oil annulus. The cylinder is provided with relief holes at E to vent any air that leaks past the piston. The lower annulus D is kept flooded with oil of good lubricating properties and all rubbing surfaces were kept well lubricated. The oil pressure in the annulus D is proportional

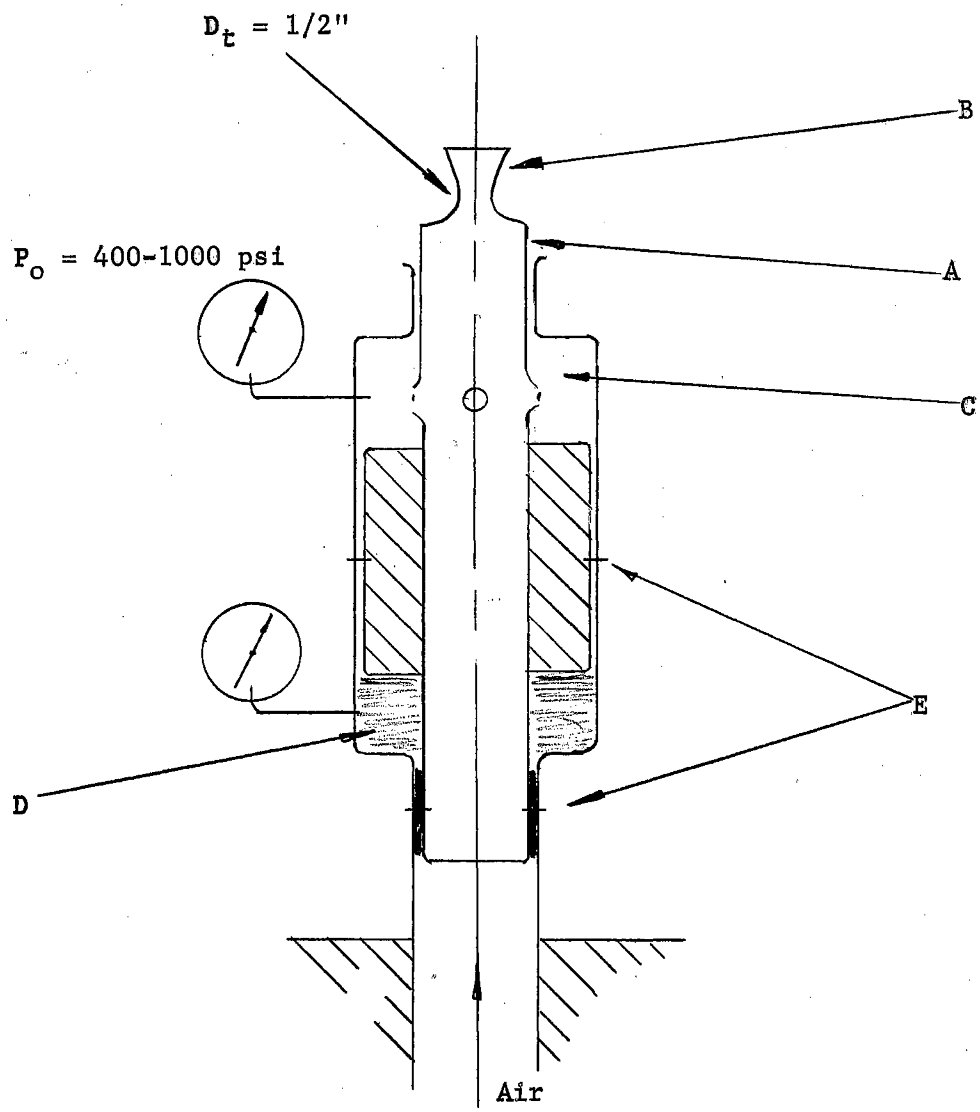

Fig. 4. Fraser, Connor and Coulter (1946), Fraser and Rowe (1954), Fraser, Rowe and Coulter (1957) Apparatus

to the axial thrust reaction and this was measured by means of a Bourdon tube gauge. The gauge was isolated from the oil in the annulus by means of a diaphragm in order to keep the hydraulic fluid free from air. The apparatus was used with air from reservoir pressures at between 400 and 1,000 psi and discharged through nozzles of 1/2-inch diameter throat. Thrusts varied from 100 to 300 pounds. The standard deviation of a single thrust observation (based on repeats) was ± 4.0 pounds, or somewhat more than $\pm 1.0\%$ of the maximum thrust values. With a few repeats, an average value with an error of $\pm 1/2\%$ could be obtained.

Ashwood (1956) (2) has employed a novel design that incorporates two free joints. (Figure 5). A vertical pipe hangs from an upper rigid support and contains the two hinges. Each hinge consists of two flanges pinned together so that they will rotate about an axis perpendicular to the axis of the pipe. About .005-inch clearance is left at the ends of the adjoining pipes to allow free movement over a limited arc and the resulting leakage is tolerated. The nozzle is mounted to discharge horizontally from the foot of this doubly hinged pipe and a cable supports the nozzle so that there is no bending moment in the vertical pipe. Guide rollers prevent any lateral movement and the reaction is measured by a spring balance. Air is supplied from a continuous source at pressures up to about 150 psi. Nozzle throat diameters varied from about 1 inch to 2 inches and the maximum force measured is of the order of 300 pounds. No figures were quoted in the published work and estimates of accuracy

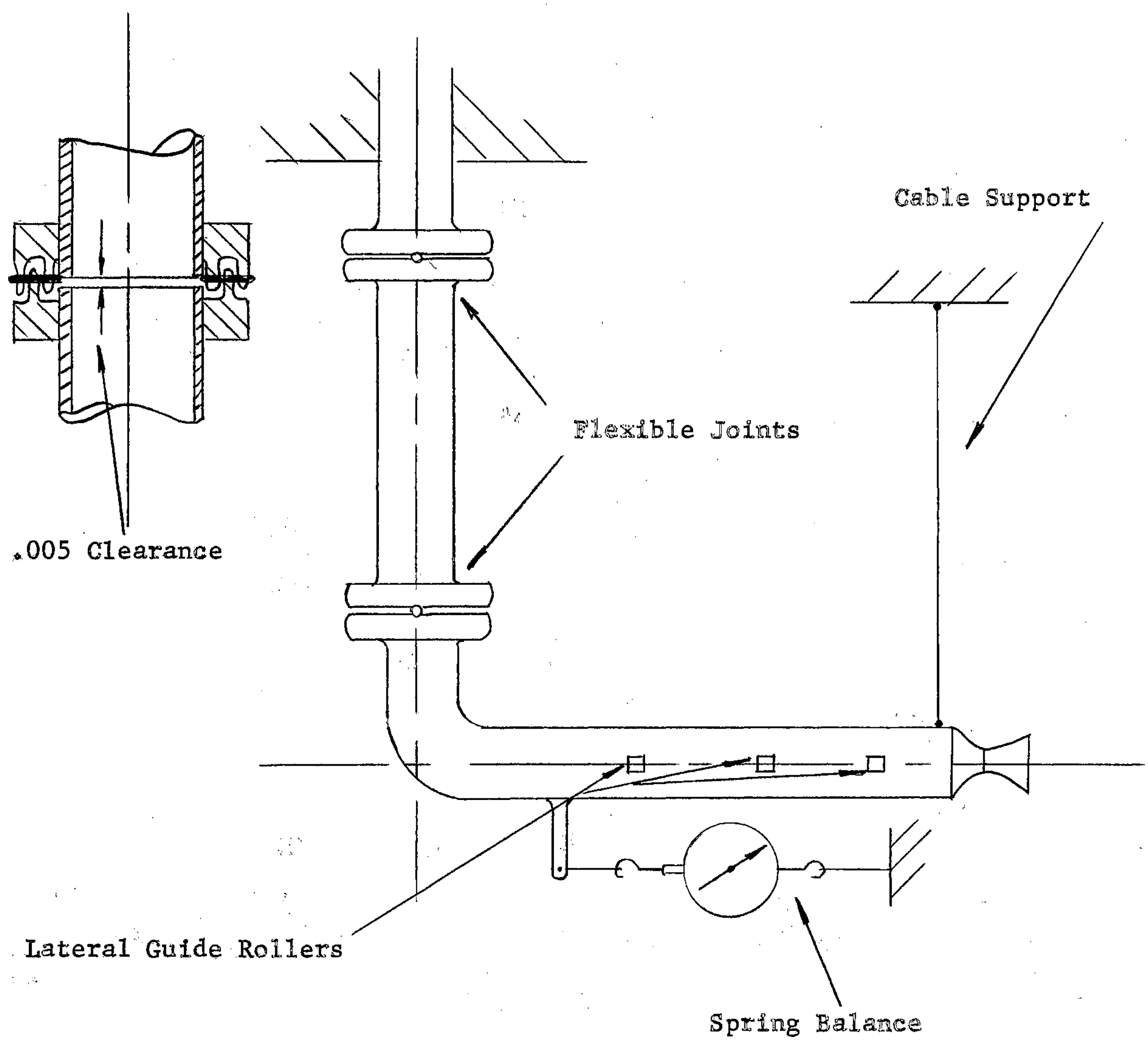

Fig. 5. Ashwood (1956) Thrust Measurement Device

could only be scaled from the graphs. The sensitivity was at least ±1/2 pounds but the standard deviation of repeated results was little better than ±1%.

Rowe (1957) (3) has designed a thrust measuring apparatus providing for partial counterbalancing of the thrust load so that the sensitivity is improved. (Figure 6). Air is admitted to a short horizontal pipe supported rigidly at its ends. The center length of this pipe is surrounded by a thick-walled steel cylinder with a very small clearance and supported in ball races so that it is free to rotate about the pipe. An annulus is cut in the center of the cylinder and connects to a radial hole. Radial drillings in the horizontal pipe communicate with the annulus. An elbow leads from the radial hole in the cylinder to a vertical stand pipe at the top of which the nozzle is mounted. Rotation of the cylinder is prevented by a support under the elbow which includes a hydraulic pressure capsule to record the thrust force. The greater part of the thrust is counterbalanced by weights on a horizontal arm so that the pressure capsule records only the small difference and may thus be very sensitive. Calibration is accomplished by hanging weights from a knife edge set on the thrust axis. Air was supplied from pressures between 10 and 1,000 psi (maintained by a pressure controller) and the nozzles were generally of 1/2-inch diameter throat. Thrust values ranged from about 3 to 300 pounds. The sensitivity is ±0.2 pounds and this can be improved to about ±0.05 pounds when thrusts less than 30 pounds are to be measured. The standard deviation of a single observation (based on repeats) is

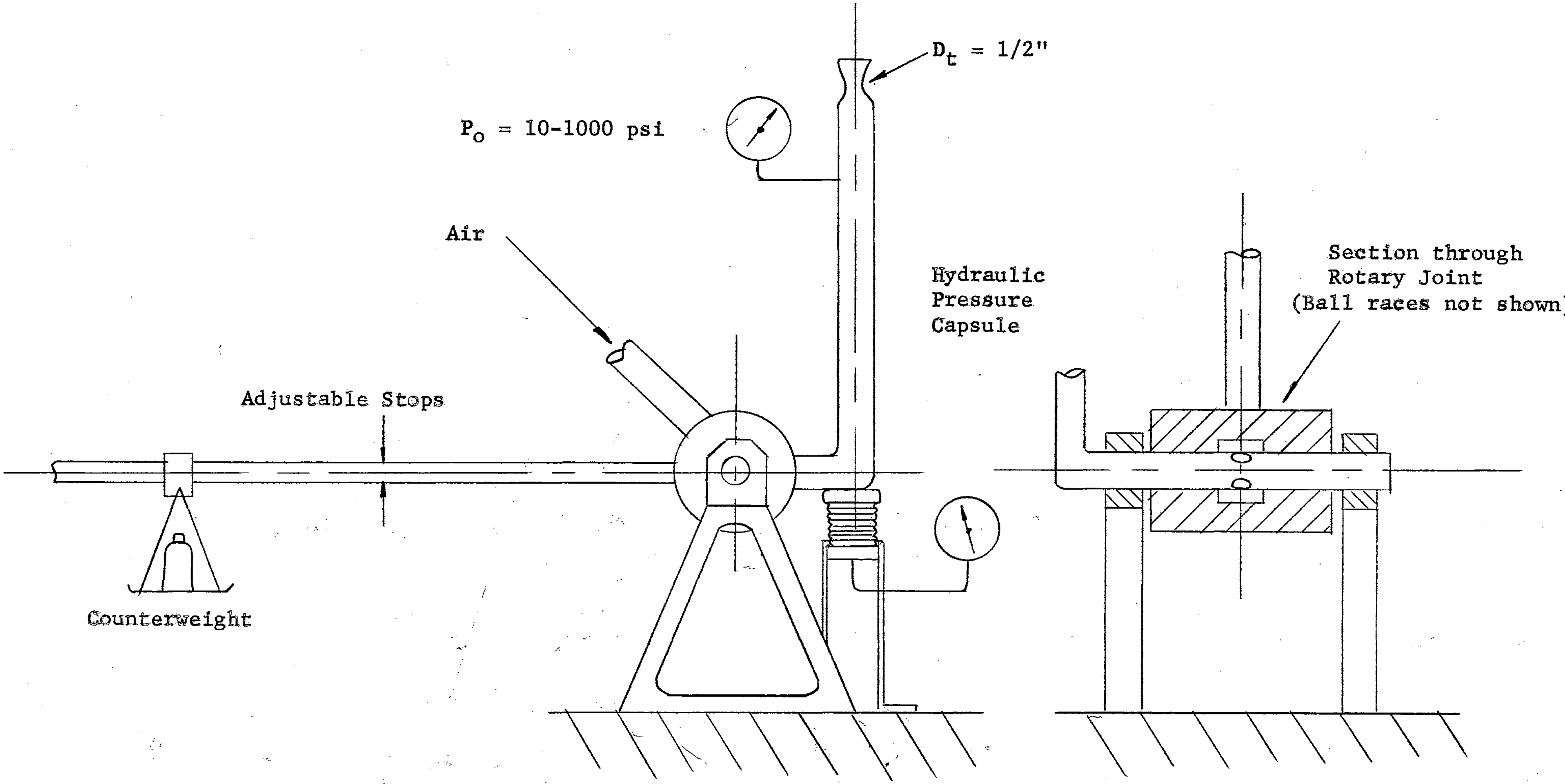

Fig. 6. Rowe (1957) Hydraulic Measurement Method

about ± 1.0 pounds or $\pm 1/3\%$ of the highest values. With a few repeats, an average value with a standard deviation of -0.1% of the larger values can be obtained. The major obstacle to improvement of this accuracy is measurement of the reservoir pressure.

Some of the disadvantages of the two previous methods are overcome by combining their advantages. (Type c). If the supply pipe is made very flexible, changes in its stiffness will be a small fraction of the measured thrust. When the supply pipe is very flexible, the nozzle must be supported so that it can move freely along its thrust axis restrained only by the measuring device. Sometimes a gauge connection may add some rigidity to a system otherwise allowing free movement. Inherently, this method combines some of the disadvantages of the previous methods and these ultimately limit its sensitivity which appears to be less than possible with free movements alone. Very simple apparatus can be built around this method and it is particularly suitable for preliminary work or for ad hoc thrust values wanted quickly without high precision.

Stanton (1926) (6) used a nozzle fitted to a free piston in order to discharge to sub-atmospheric pressures. (Figure 7). Air was discharged downwards through a nozzle which was part of a piston sliding in a cylinder which led to a suction pump. The piston assembly was supported from the arm of a balance and air was supplied through two loops of a flexible rubber hose. The differential air pressure over the piston must be added to the recorded thrust. The reservoir pressure was 45 lb/in.^{2} (absolute) and the reservoir pressure

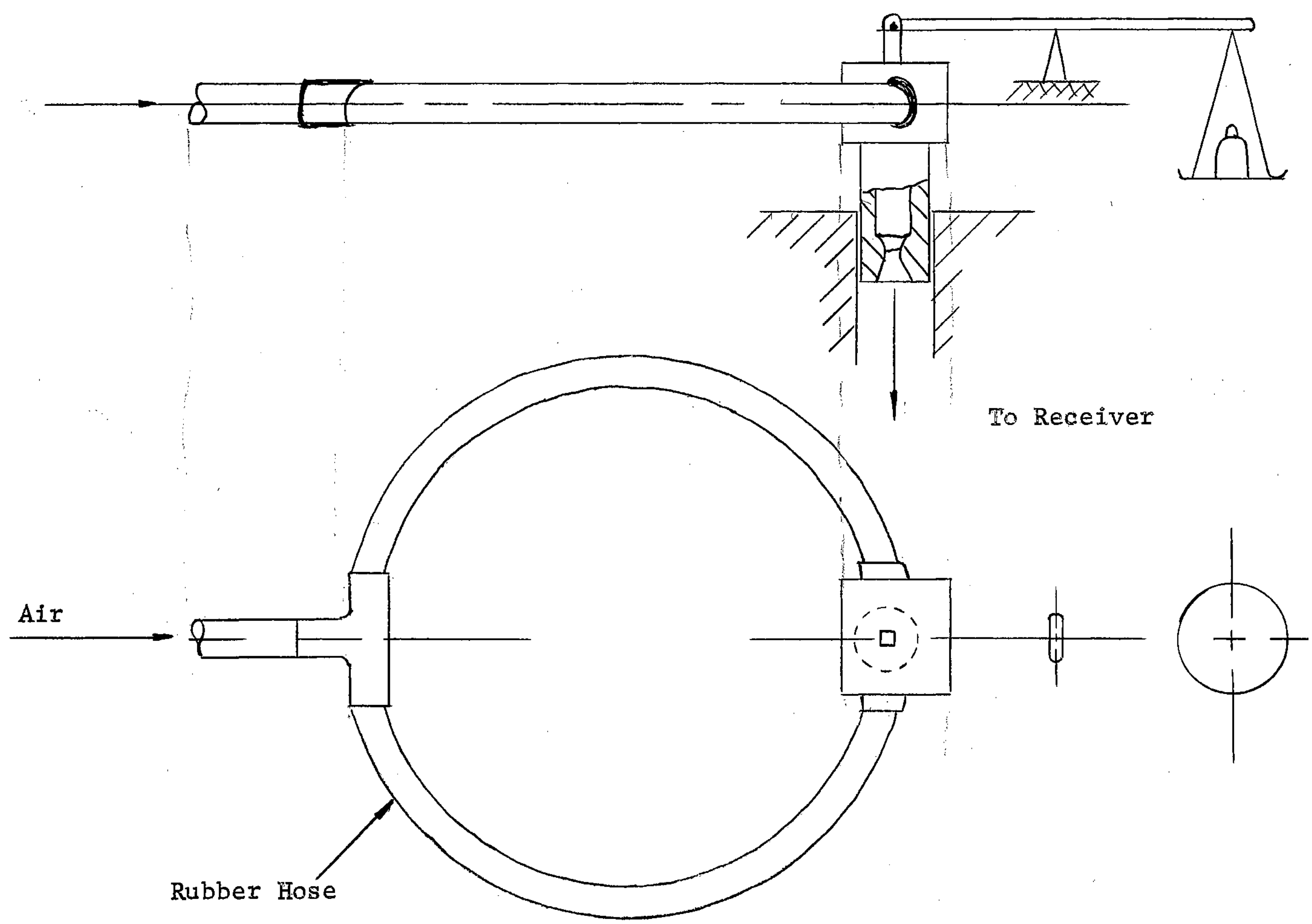

Fig. 7. Stanton (1956) Thrust Apparatus

varied from 4 to 10 lb/in.^{2} (absolute). The nozzles were of approximately 1/2-inch diameter throat and thrusts of about 12 pounds were recorded. The accuracy was reported as better than $\pm$1.5%.

Hubble and Sinclair (1956) (3) describe a small thrust rig that allowed free movement except for the coiled copper feed pipe and pressure gauge connection. (Figure 8). The nozzle is attached to one end of a balance beam and discharges downward transmitting the thrust to an electrical force transducer below the other end of the beam. The nozzle was supplied with hydrogen peroxide up to the reservoir pressures of 650 psi and the nozzles had throat diameters of the order of 0.1 inch. The maximum thrust recorded was about 12 pounds. The sensitivity of the balance was about $\pm$0.3 pounds but the standard deviation of repeated observations was approximately $\pm$0.2 pounds or $\pm$1.5% of the maximum value.

In much development work, it is only necessary to measure the improvement in thrust of one nozzle over some standard. By supplying two nozzles from a common reservoir and discharging them in opposite directions, (Type d), only the difference in the thrust need be measured. This method combines the very great advantage that reservoir pressure need not be measured with great precision as it can generally be considered to be the same for both nozzles. On the other hand, the two throat areas must be nominally the same and the exact areas must be measured with great precision. The problem of measuring the thrust difference is essentially the same as that of measuring the total thrust. A common arrangement is to mount the supply pipe vertically as a pendulum

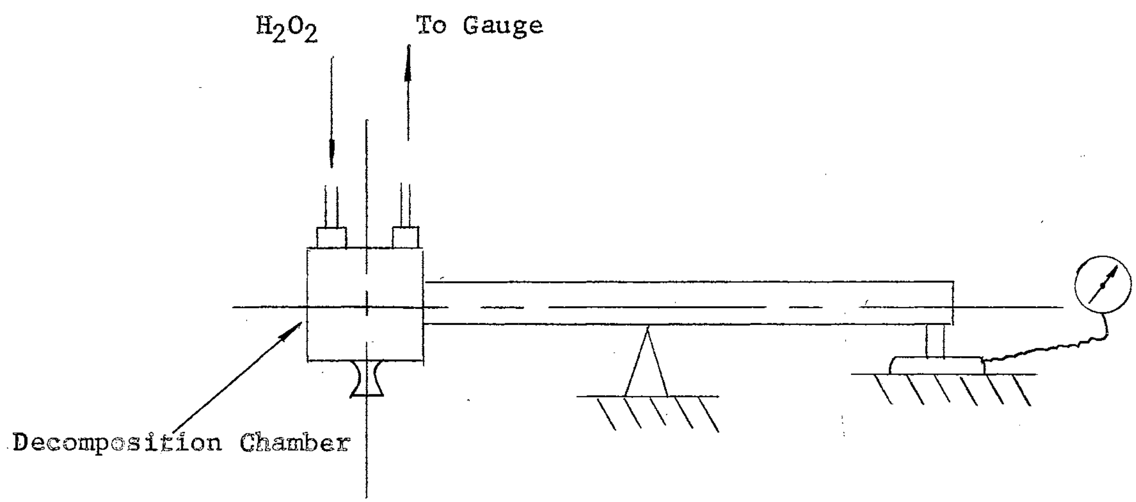

Fig. 8. Hubble and Sinclair (1956) Device

and to arrange the two nozzles to discharge horizontally from the free end of the pendulum. The suspension of the pendulum and its supply with gas can be by any of the three previous methods. The main advantage of thrust comparison is the insensitivity to error in reservoir pressure measurement and the reduced scale over which measurements are made.

Several of the authors state that further designs should investigate improved methods for reservoir pressure measurement, labyrinth glands sealing method, and thrust measurement calibration procedure.

No laboratory method has been found in the literature which considered measurement of non-axial thrust components with the resulting ability to both measure and locate the thrust vector. This is desirable in many rocket nozzle applications.

CHAPTER III

THRUST FACILITY LAYOUT

The School of Mechanical Engineering had felt the need for expanding their gas dynamic facilities. This past fall a decision was reached to appropriate money for the specific purpose of broadening two areas. One of these was high speed research through the construction of a two-dimensional supersonic wind tunnel. The other area was concerned with thrust nozzle application to rocket propulsion. This thesis is primarily concerned with the design development of the basic apparatus to be used in the latter area.

The primary limitation on the development of these projects lay in the existing compressor size. Therefore this became the chief design parameter. The location for the gas dynamic laboratory was chosen to be near the east wall south of the subsonic wind tunnel in the Mechanical Engineering Laboratory. The space was limited forcing the decision to tear out part of the east wall and to build an adjoining machinery room. The 32' x 15' machinery room was constructed for the specific purpose of housing all of the equipment necessary to process the air for use in the thrust stand and wind tunnel. The machine room layout is shown in Figure 9, including the engine, compressor, intercooler and aftercooler combination, air dryer, filters, and one-way valve. For specifications and

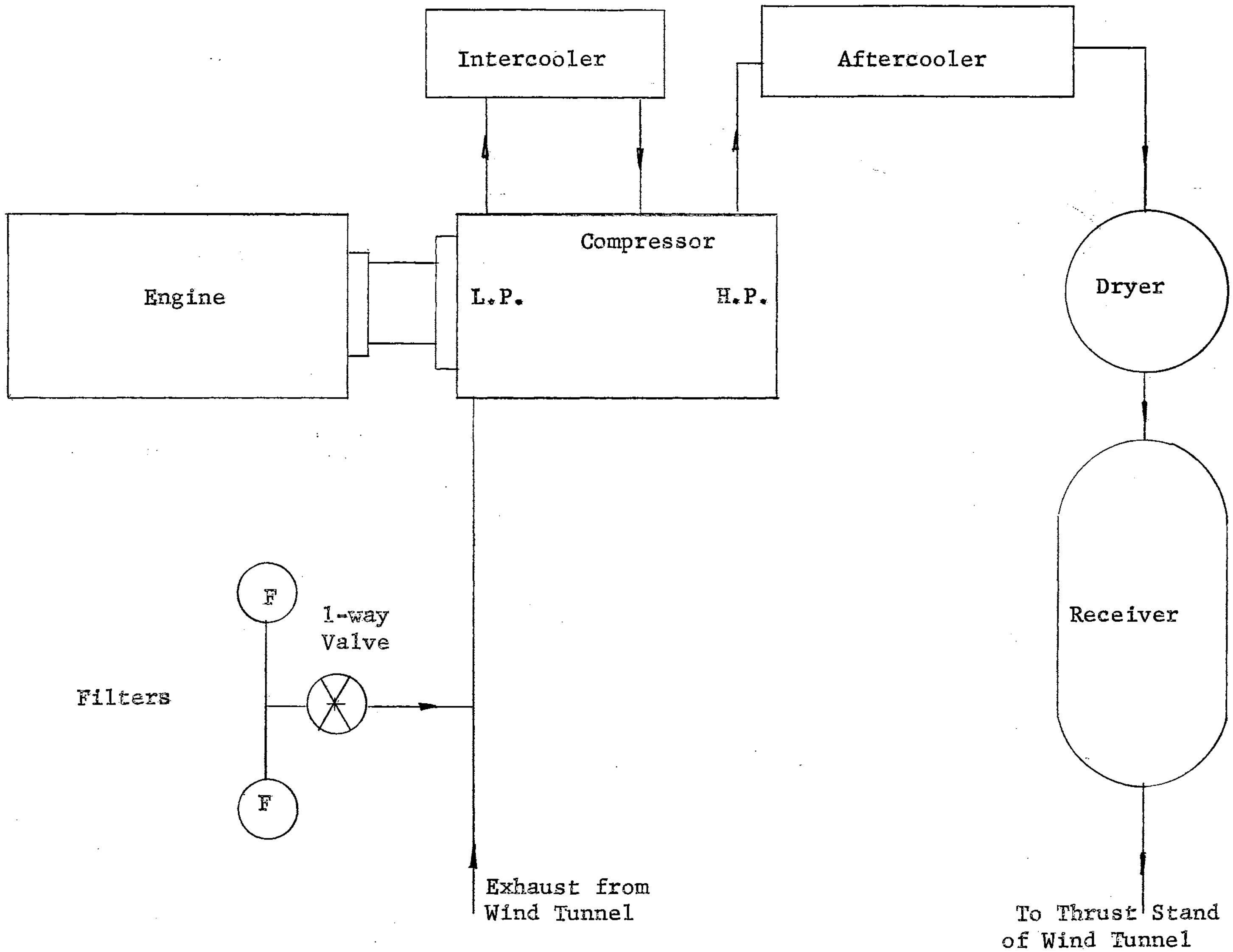

Fig. 9. Machinery Room Layout (Schematic)

manufacturers data see Appendix A. A one-way valve was designed for the air supply inlet to the compressor. (Figure 10). The valve was designed enabling regulated pressure drop across the valve of from zero to five pounds per square inch. The method of securing fresh air for the compressor is to create a partial vacuum in the line, thus sucking the air through the filters. This one-way valve furnished a fresh air control method and also enabled a variable back pressure for the second throat of the wind tunnel to be maintained.

The air from the receiver flows from the machinery room into the laboratory in a ceiling-high pipe. A tee was installed in this line allowing flow to either the test stand or the wind tunnel. As equipment and instrumentation are limited only one of these can be operated at a time. The wind tunnel operation sends the air through a return line to the air processing stages. (Figure 9).

When the valves are adjusted to cause the air flow to be diverted to the nozzle test stand (Figure 11), the compressed air flows vertically downward to a gate valve (throttling control). This valve allows a little finer stabilization of the flow before letting it round the bend to the flow metering nozzle. This nozzle was designed according to ASME Flow Measurement Code 1956 (Appendix B). The flow metering nozzle was mounted in the three-inch pipe between two flanges and proper instrumentation was installed according to the ASME Code previously mentioned. Plate I shows this flow metering nozzle.

Upon passing through the flow metering nozzle the piping enters the thrust stand room. The room was constructed out of a walk-in

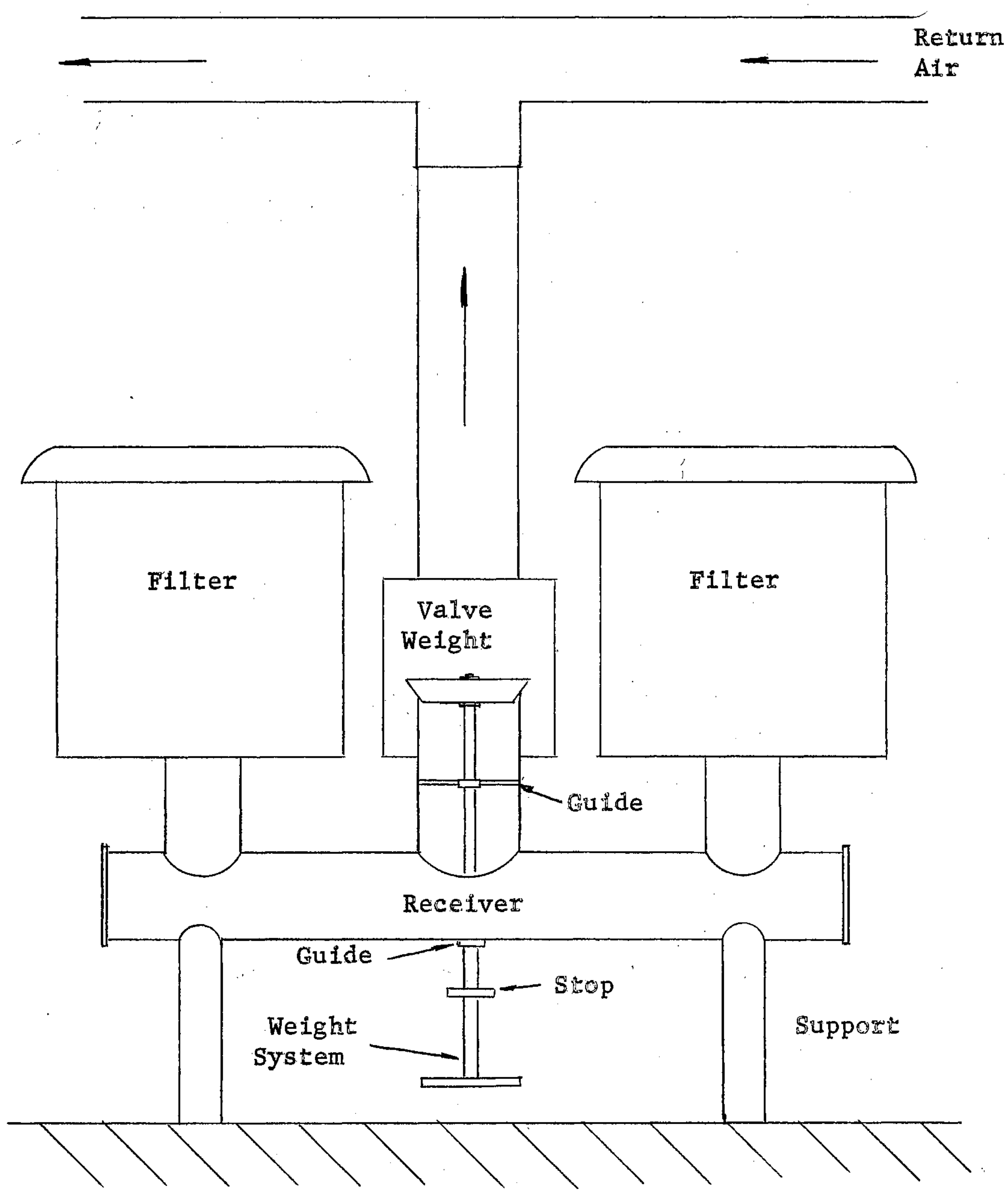

Fig. 10. One-way Valve

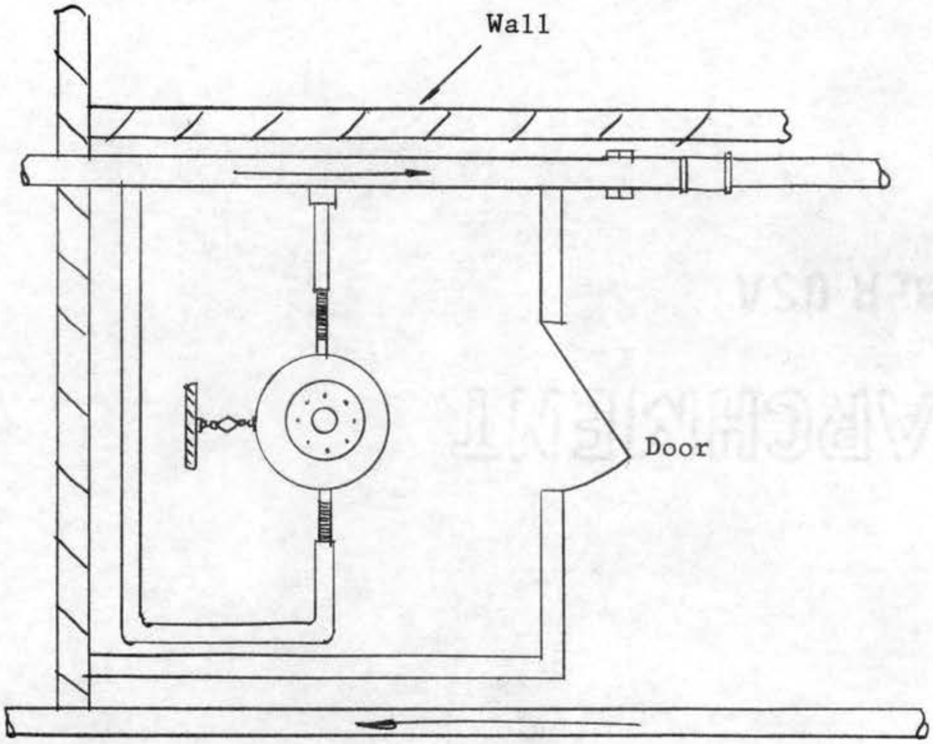

Top View

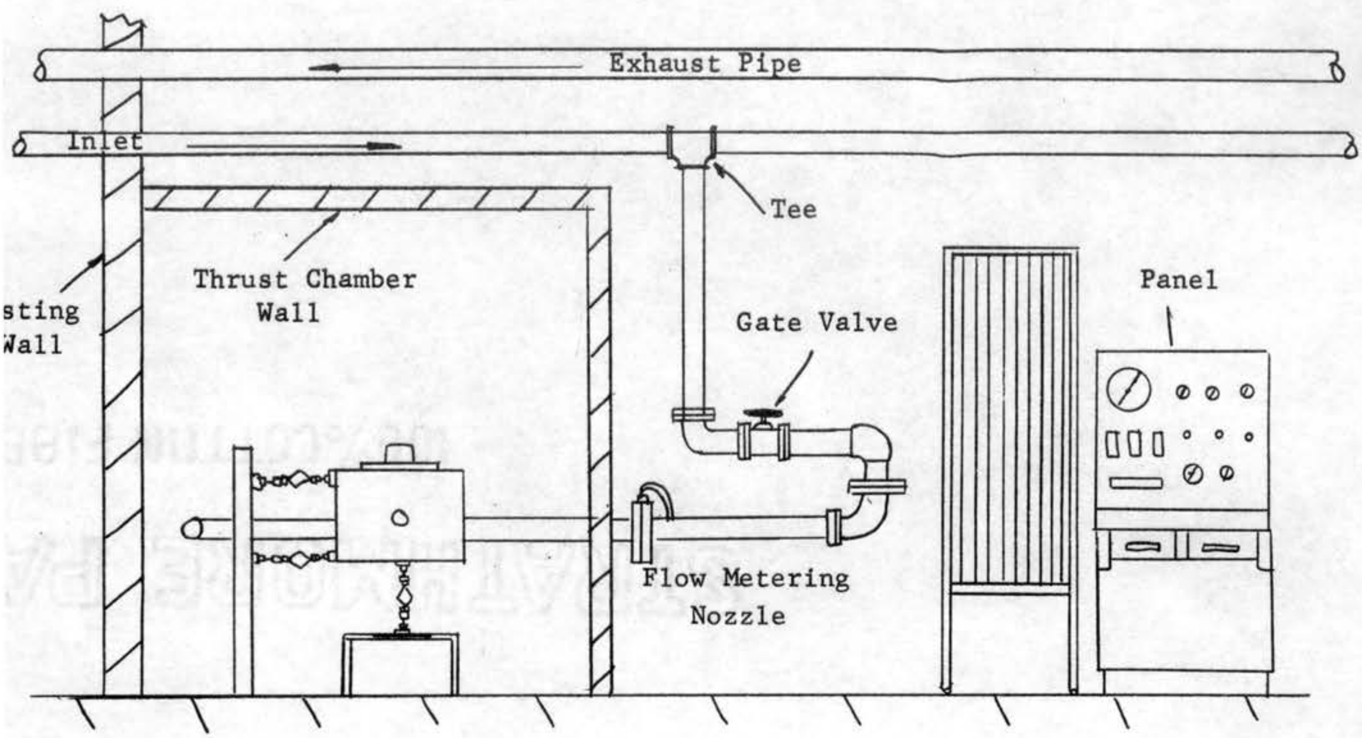

Fig. 11. Piping Layout

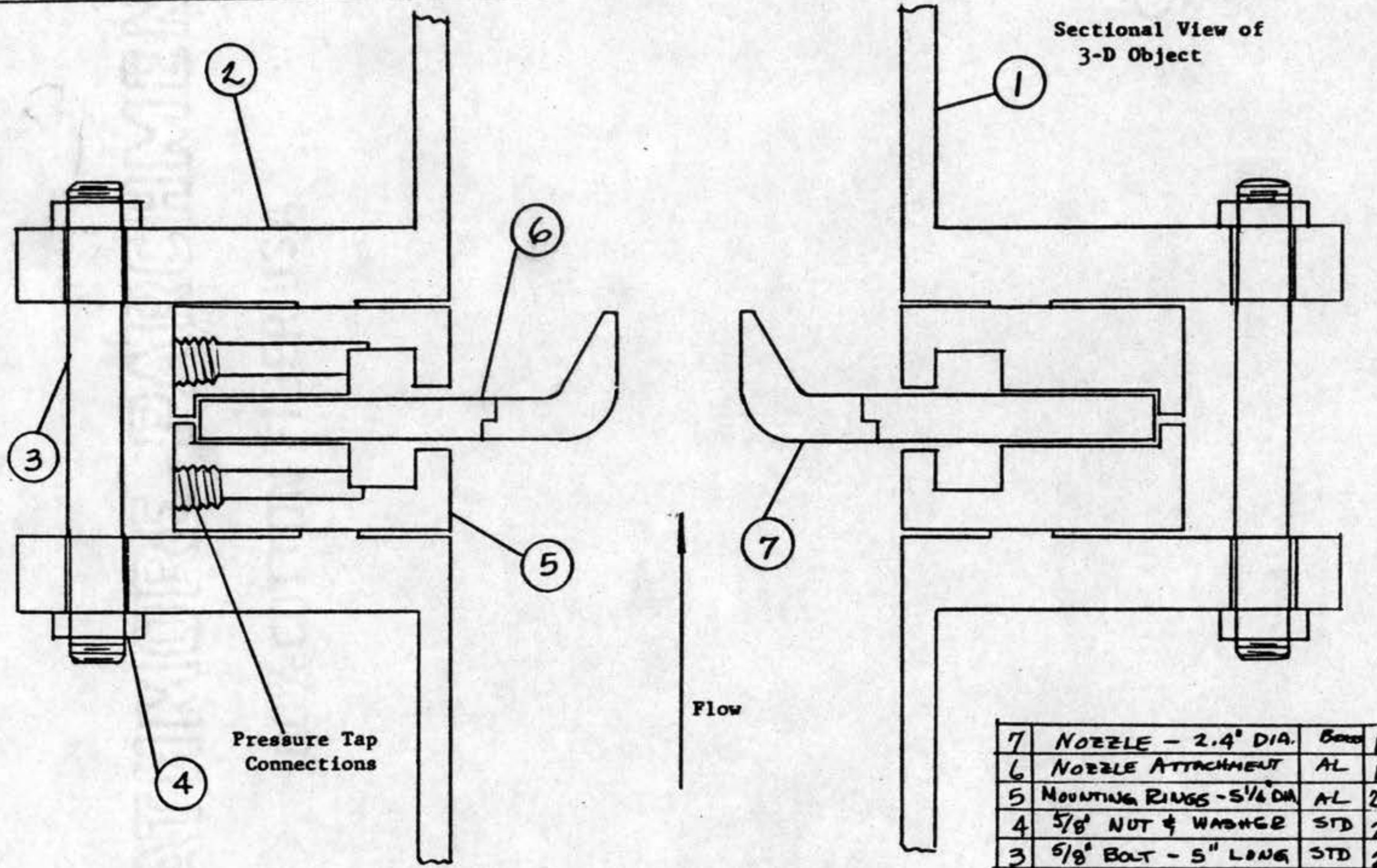

7	NOZZLE – 2.4" DIA.	[illegible]	1
6	NOZZLE ATTACHMENT	AL	1
5	MOUNTING RINGS – 5 1/4" DIA	AL	2
4	5/8" NUT & WASHER	STD	2
3	5/8" BOLT – 5" LONG	STD	2
2	PIPE FLANGES	STD	2
1	40 GAUGE PIPE 3" DIA	STD	1
NO	PART DESCRIPTION	MAT'L	REQ.

OKLAHOMA STATE UNIVERSITY
FLOW METERING NOZZLE
GAS DYN. LAB RESEARCH PROJ [illegible]
DWG: GRS SCALE: 1=1 CHK: G.W.Z

PLATE I. FLOW METERING NOZZLE

storage icebox which proved to be an inexpensive but satisfactory insulation room for enclosing the thrust stand and confining the sound of the issuing jet. Inside the thrust stand enclosure the incoming air was split into two flows carried in two-inch pipes with flexible sections of twenty-inch length joining to the plenum chamber. These join into the plenum changer 180° apart on the chamber circumference. These special flexing sections were used to provide enough flexibility to isolate any extraneous pressure forces, vibration, or rigidity, which might otherwise affect the thrust measurement.

The thrust stand plenum chamber was designed using a twelve inch diameter, schedule forty, pipe as the basic component. The heads were designed using ASME "Unfired Pressure Vessel Code" 1956 (Appendix C) with plate steel as the material. (15). Steel was used because of availablility, ease of assembly and strength considerations. The heads were attached by welding a 3/8-inch fillet weld around the outer circumference of the plenum chamber. The bottom head was only plate steel with no machining necessary. The top head had a 2½-inch diameter hole in its center and eight equally spaced 1/4-inch bolt holes were drilled on a six-inch diameter pattern to enable nozzle mounting. The plenum chamber is shown in Plate II.

A typical axi-symmetric nozzle was designed for preliminary operation of the thrust nozzle test stand. The conical nozzle was designed for obtaining the maximum Mach number from the compressor limitations with atmospheric back pressure. This nozzle is shown in Figure 12a and b,

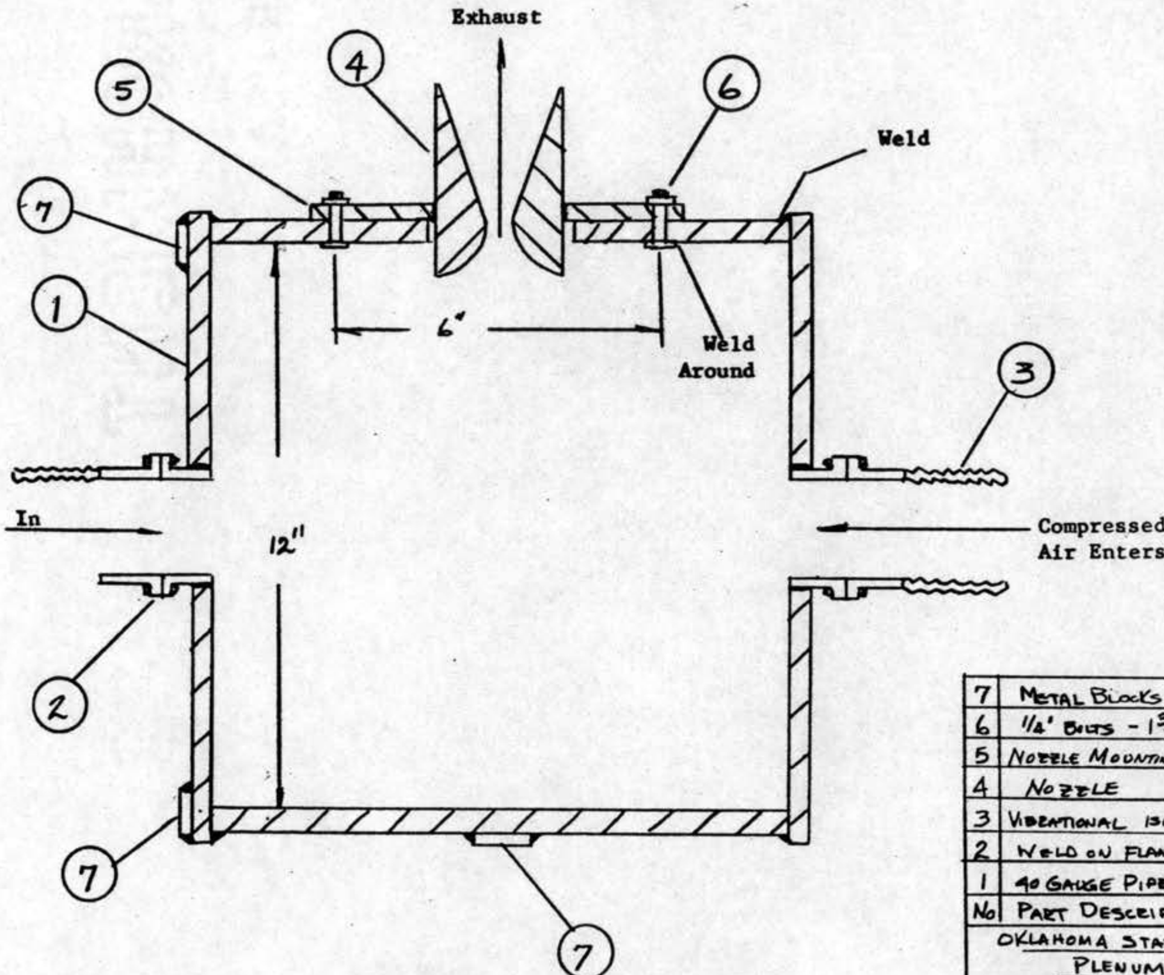

No	Part Description	Material	Req
7	Metal Blocks 2" x 2" x 1/2"	STD	3
6	1/4' Bolts - 1 3/4" Long	STD	8
5	Nozzle Mounting Plate	STD	1
4	Nozzle	BRASS	1
3	Vibrational Isolator - 2"	STD	2
2	Weld on Flange 2" DIA	STD	2
1	40 Gauge Pipe 12" DIA.	STD	1

OKLAHOMA STATE UNIVERSITY
PLENUM CHAMBER
GAS DYN. LAB — RESEARCH PROJ. 171
DWG: GRS — CHK. G. W. Z.
SCALE: 1 = 4

PLATE II. PLENUM CHAMBER

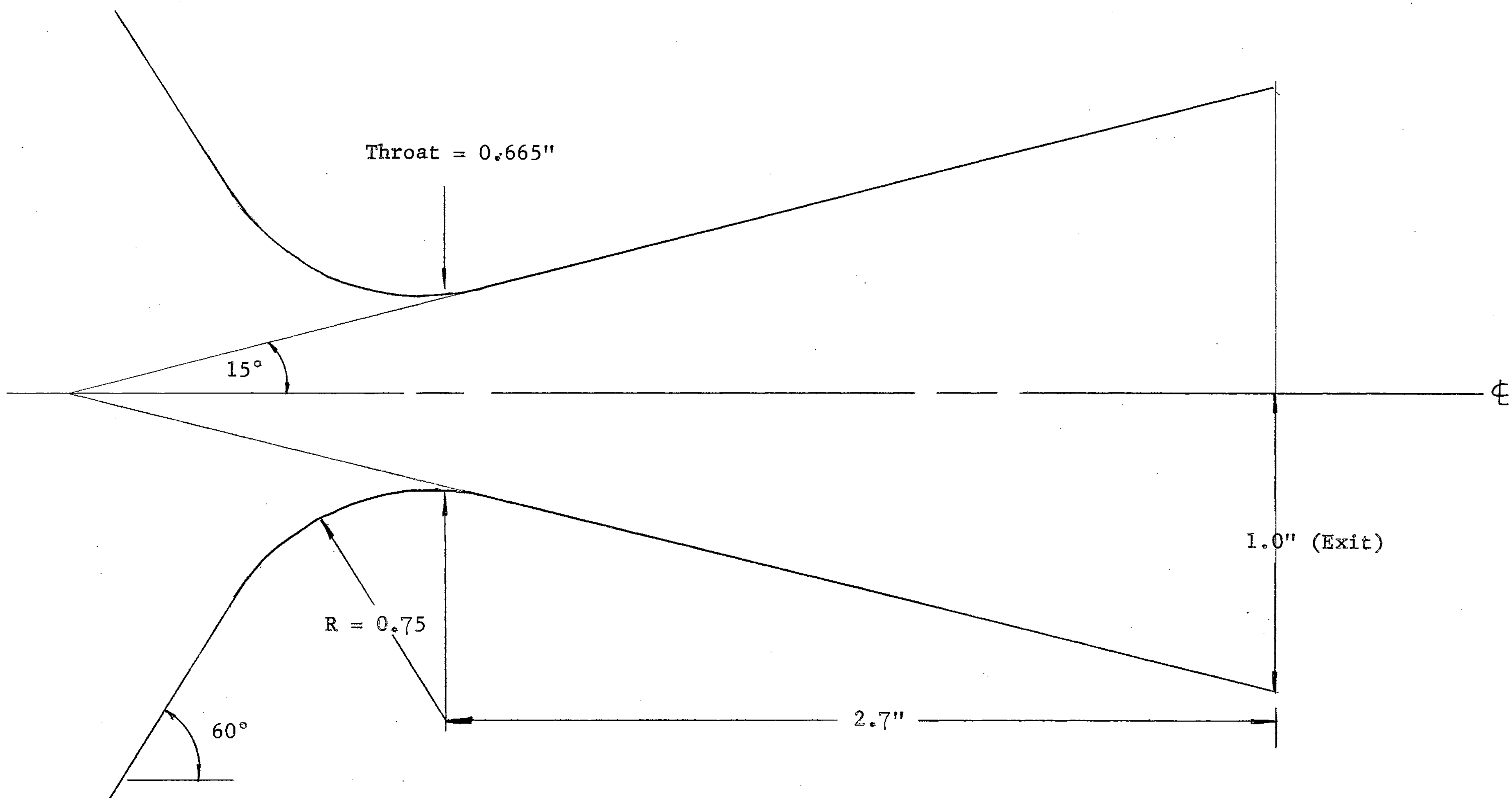

Fig. 12a. Typical Nozzle

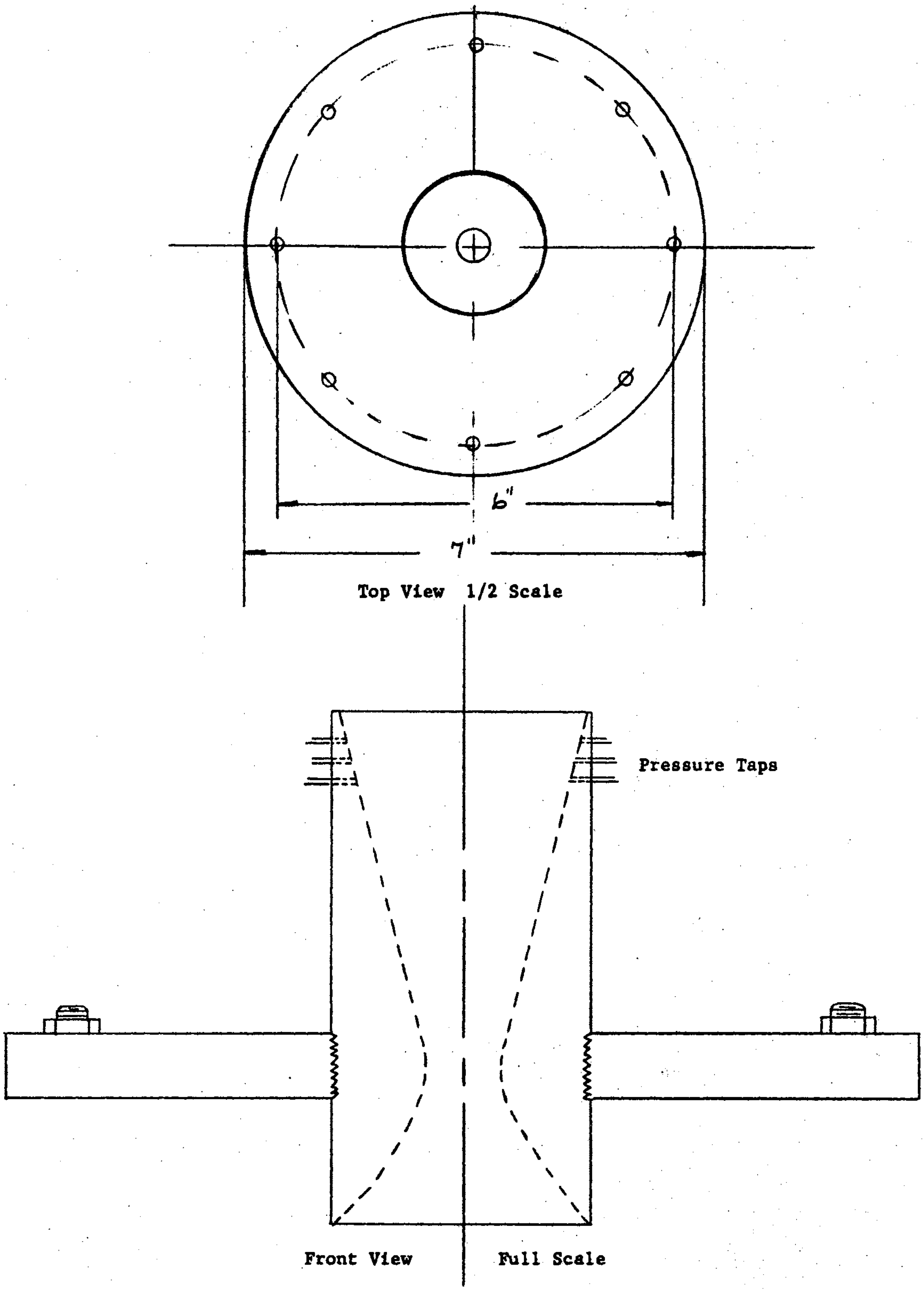

Fig. 12b. Typical Nozzle

and calculations are given in Appendix D.

Upon the completion of all the thrust stand components, final assembly should be undertaken. The ejector system whose detailed design is discussed later should then be mounted in place. Pressure taps should be located as suggested. (Figure 12b). All thrust measuring equipment should be calibrated and installed for operational use.

CHAPTER IV

ROCKET NOZZLES

In this section consideration will be given to basic types of rocket nozzles and several variations developed. Special emphasis will be placed on those nozzles particularly applicable to solid propellant rockets. Since the solid-propellant motor permits a comparatively compact package, missile design engineers tend to press this advantage to the utmost. In some instances even the available length for nozzles is fixed, and it is desirable for the designer to get the maximum performance within the space limitations. There are several variables which affect the length of the nozzle. These include throat diameter, the radius of approach, the exit angle, and the expansion ratio. The extent to which variations in each of these affects performance has been explored by a number of investigators. (2).

Three general classes of rocket nozzles will be considered here--the basic conical nozzle, the Foelsch design contour nozzle, and the Rao nozzle, a modified contour nozzle.

Conventional 15° conical nozzles used on solid-propellant motors represent from 15% to 30% of the total motor length. Existing nozzle design theories indicate that these nozzles can be shortened by 25% to 35% in some cases. Therefore, a minimum-length nozzle design is of prime importance to rocket motor design. Comparison of nozzle designs for solid-propellant motors on a theoretical basis is complicated by the several variables that have not been fully evaluated. (10).

1). The specific heat ratio of the combustion products of solid propellants containing metallic additives is not known within one percent, as would be desired for nozzle thrust coefficient calculations.

2). The flowing fluid is not an ideal gas because it may contain up to 40% by weight, solid material. The flow in the nozzle is not isentropic because as much as 18% of the energy available in the solid fuel may be transferred to the flow gas within the nozzle.

3). Another factor associated with nonideal fluid flow which affects the thrust coefficients, and which should be considered for arrival at the optimum nozzle contours, is the boundary layer growth along the nozzle wall with its attendant skin friction. The boundary layer affects the thrust because of the wall-friction effect and because of the effective change in nozzle cross section available for the irrotational flow.

The conical nozzle is the simplest of the rocket nozzles in use today. The conventional conical nozzle theory has been tested by many groups, including Fraser, Rowe, and Coulter (5) and Durham (21), with high-pressure air as the flowing gas. In order to determine whether nozzles tested with a fluid containing a high percentage of solids would follow the theory, conical nozzles with 15°, 18°, and 25°

divergence were evaluated on solid-propellant motors loaded with a propellant containing a high percentage of metallic additives. This propellant yields an exhaust containing approximately 32% solids by weight. These tests indicate that the effect of divergence angle on the performance of conical nozzles is independent of solids content of the flowing fluids. (Figure 13). This does not indicate, however, that a given nozzle will be just as efficient with either air or high-solid-content gases. When nozzle length is not crucial and maximum specific impulse (defined as the ratio of thrust to mass rate of flow) or thrust coefficient is important, conical nozzles with less than 15° divergence, but not less than 7.5° divergence, may be used to gain as much as 1.25% in propellant specific impulse over the standard 15° conical nozzle. (11).

Let us now consider a typical conical nozzle design. Upon assuming a selection of the radius of approach and the radius aft of the nozzle throat, a choice often arises as to whether it is best to use a nozzle with a small exit angle in a space limited system, accepting a smaller expansion ratio, or whether it is better to increase the divergence loss in order to obtain a larger expansion ratio. If we ignore for the time being the differences in weight, it is possible to calculate the most desirable expansion angle for any given nozzle. Using the nomenclature in Figure 14, it can be shown that the ratio of length to the radius of throat is given by the equation

$$\frac{L}{R_t} = \frac{(\epsilon + \sec\alpha - 2)}{\tan\alpha} \qquad \epsilon = \left(\frac{R_e}{R_t}\right)^2$$

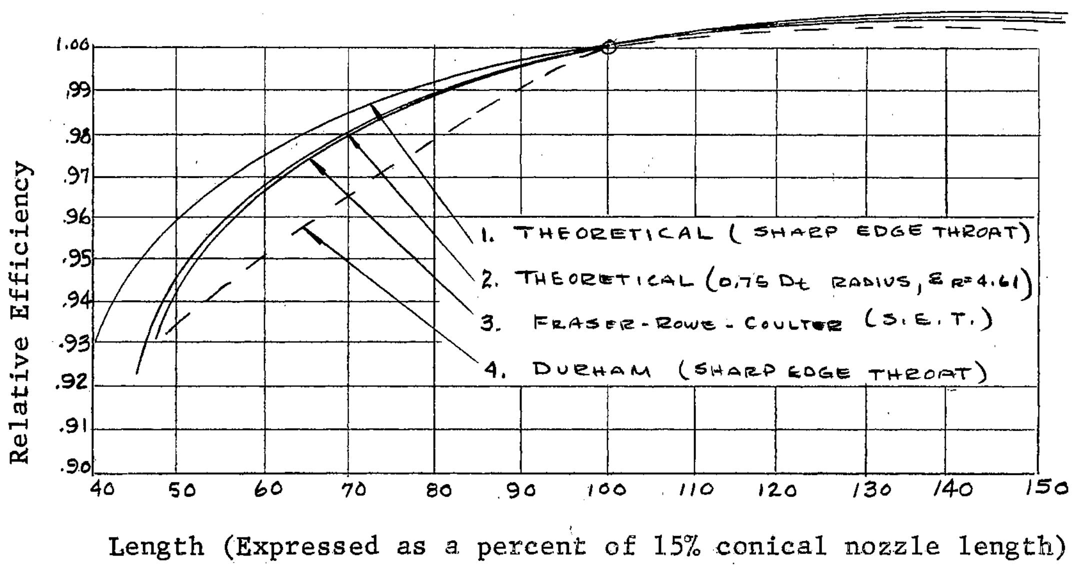

Fig. 13. Conical Nozzle Efficiency Plot

when the radius of the curvature of the approach is equal to the radius of the throat. (11). In Figure 15, the expansion ratio is plotted as a function of the ratio L/R_t for several different expansion angles. Combining these data with the value for thrust coefficient in a vacuum as a function of expansion ratio ϵ and with the correction for nozzle divergence, $\lambda = 0.5 + 0.5 \cos \alpha$, results in the data given in Figure 16. As can be seen in this graph, the optimum nozzle angle is a function of the relative nozzle length. Since for equal L/R_t ratios the nozzle with a larger exit cone angle will be heavier than the nozzle with a smaller exit cone angle, the optimum nozzle angle will be somewhat smaller than that indicated in Figure 16.

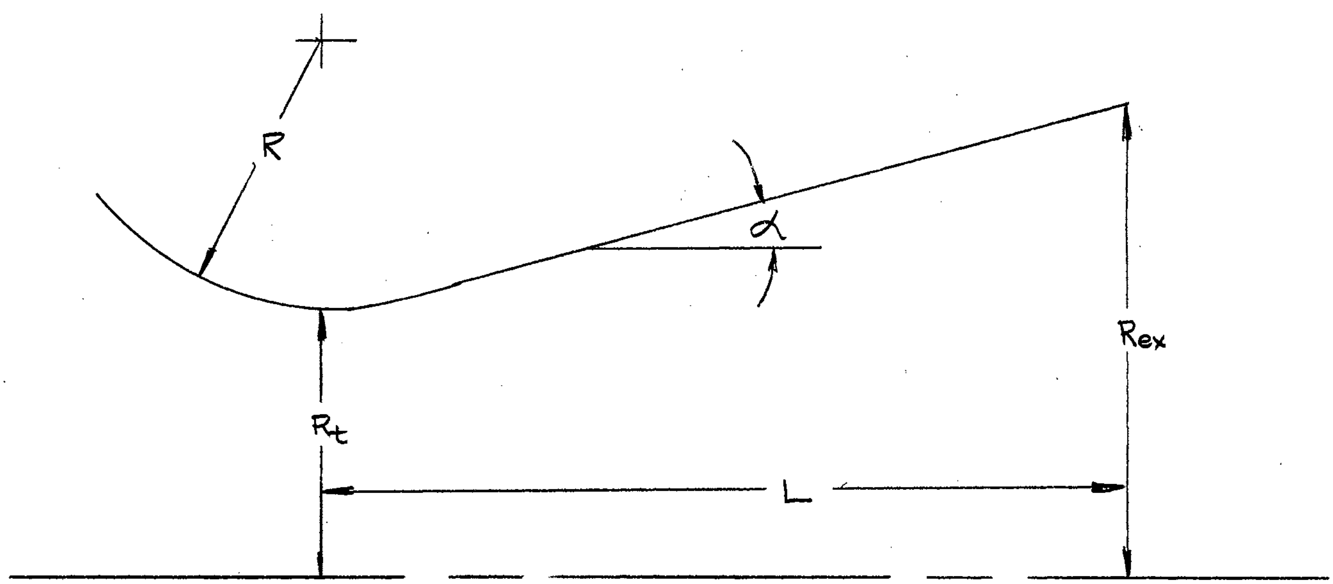

Fig. 14. Rocket Nozzle

With conical exit cones, the optimum exit angle is a function of the relative nozzle length, varying from 20° to 24° for L/R_t ratios of

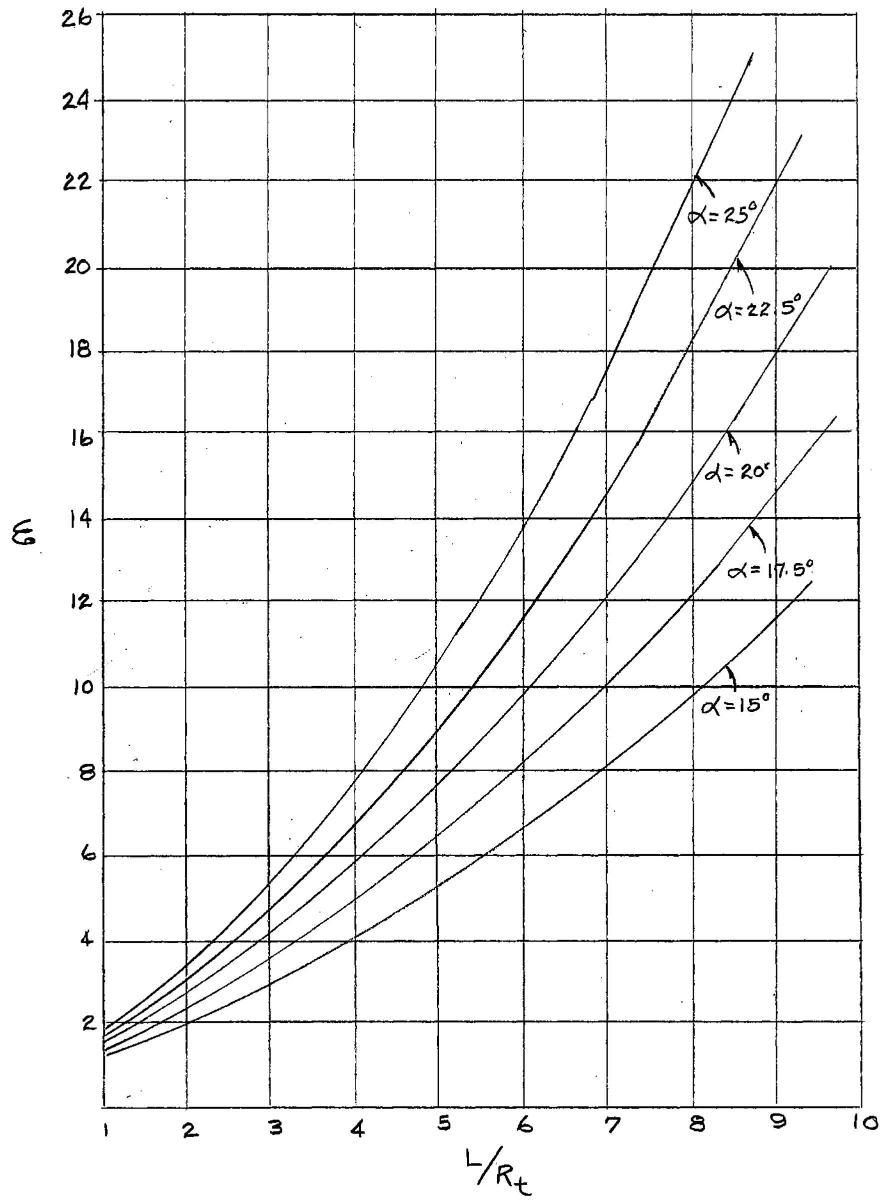

Fig. 15. Rocket Nozzle

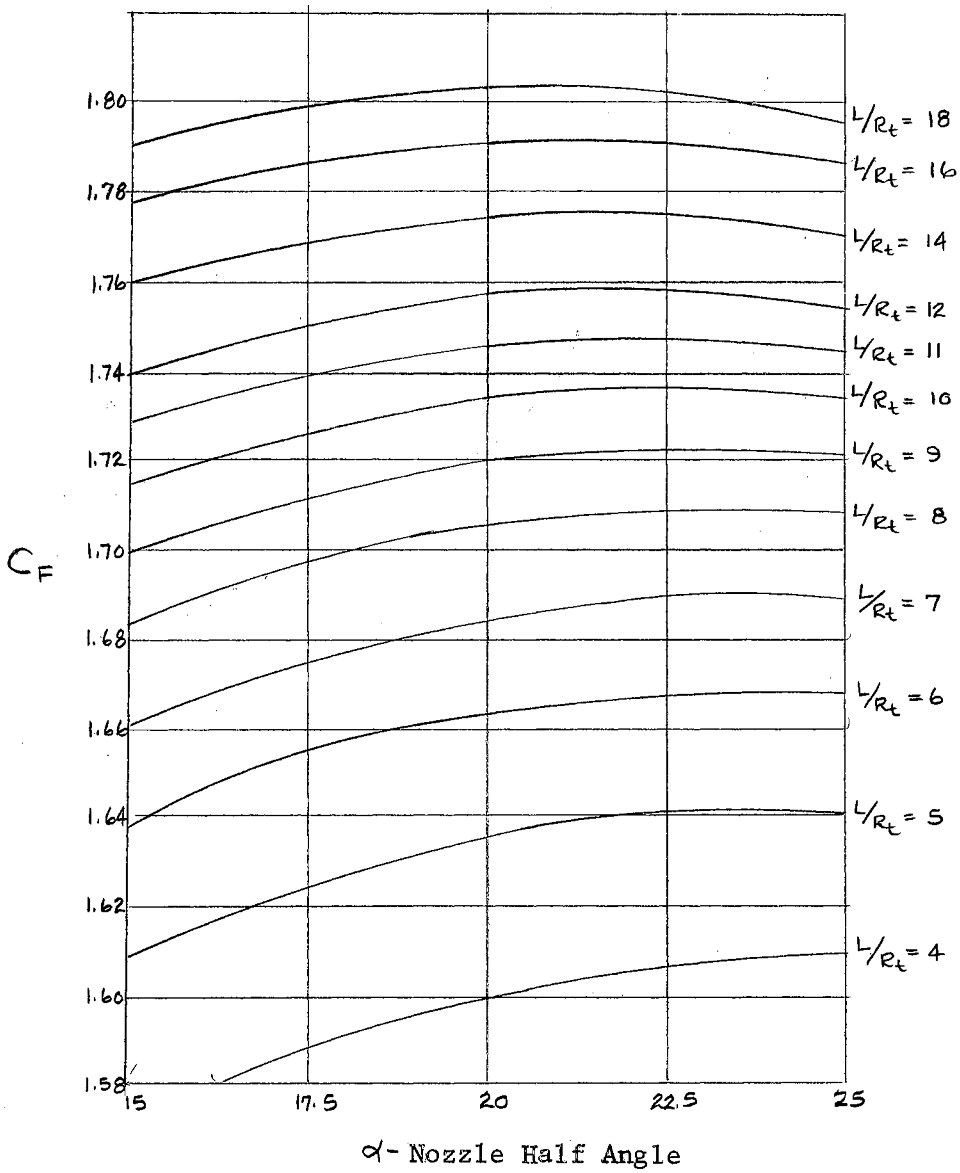

Fig. 16. Plot of C_F vs α

18 to 5 respectively. It has been demonstrated that the nozzle approach geometry has little effect on specific impulse with combustion products containing as much as 38% of non-gaseous components. (9).

Until recently the supersonic nozzles used in rocket engines have had conical expansion sections with few exceptions. There is a record of considerable nozzle research on the part of the German scientists at Peenemunde. They found no great advantage in using other more complicated shapes in the low area ratio nozzles of interest for V-2 work. This decision was probably also influenced by ease of engine fabrication considerations. The German investigations resulted in a choice of an optimum divergence angle for the supersonic conical nozzle which has been carried over into American rocket developments. (12).

The continued demand for increased rocket engine performance has resulted in a definite trend to higher exhaust area ratio nozzles for engines operating at high altitudes where the larger nozzle is most effective in increasing engine performance. Conical nozzles, when extended to higher area ratios, become unwieldy in both length and exit diameter. The engine is harder to handle, its weight is increased noticeably, and the nozzle experiences larger stress loads which compound fabrication problems. The increase in weight and stress loads is of added importance if one considers using the engine for thrust vector control by swinging (gimbaling) it on its mount. Increased engine and moment of inertia increase the power required to move the engine and thus add to the weight and complexity of the thrust vector control system.

As a result of the foregoing considerations it appears desirable to minimize the nozzle length of the large high performance rocket engine. One immediately thinks of increasing the divergence angle of a conical nozzle in order to accomplish this objective. However, as the divergence angle is increased, the momentum loss, due to non-axial fluid flow and the associated loss in performance, outweighs any advantages from decreased weight and moment of inertia. Even with conical nozzle design there is a loss in performance of about 1% due to the partial flow divergence from the axial direction in the nozzle exit plane.

Today engineers are trying to design short, high area ratio, supersonic nozzles having performance equal to or superior to present conical nozzle motors at design altitude. In such a design it was necessary first to expand the nozzle more radically from the sonic throat (as compared to an ideal nozzle) and then more severely over-turn or straighten the flow into approximately axial flow at the exhaust.

Kuno Foelsch at the J. P. L. Cal-Tech symposium in 1946 proposed an analytical design method for supersonic nozzle design based on the fundamental ideas used by Prandtl and Busemann in solving the problem graphically. Foelsch's report showed that the coordinates of the contour of an axially symmetric nozzle, as well as of any streamline in the nozzle's flow, may be immediately determined from two simple equations. The first part of the report deals with the derivation of the equations for the transition curve by which the conical source flow emanating from the sonic section is converted into a parallel and uniform flow. In the second part of the report, the spherical sonic flow section is adjusted to a plane flow section at the throat of a nozzle. (7).

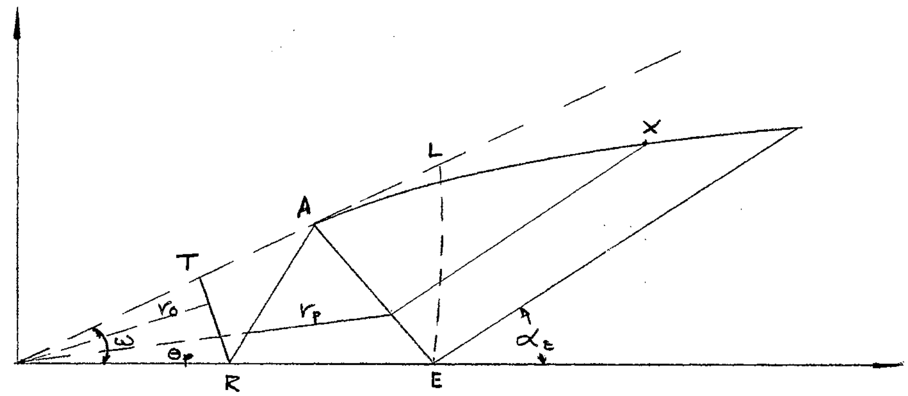

Conversion of Radial Flow into Parallel Flow

A two-dimensional flow field in which the velocity is everywhere supersonic can always be represented approximately by a number of small adjacent quadrilateral flow fields in each of which the velocity and pressure are constant. These quadrilaterals must be separated by lines representing waves in the flow; changes in velocity and pressure through any wave can be computed. By increasing the number of small areas into which the complete flow field is divided, the accuracy of this approximate solution may be increased without limit. This constitutes the "method of characteristics" solution. This method may be applied to the graphical computation of flow in a supersonic nozzle, with the particular aim of producing uniform supersonic flow at the end of the nozzle.

In a real fluid some viscous effects must be present, but it can be shown that they are, for the most part, confined in a thin layer next to the walls of the flow, called the boundary layer. The real flow then essentially consists of a core of nonviscous flow, and thin layers of retarded flow along the wall. It can be shown that the perfect fluid core behaves as though it were flowing between walls which lie somewhere in the boundary layer, inside the physical wall. These "effective walls" are displaced inside the true walls by certain distance, less than the boundary-layer thickness, called the "displacement thickness." The displacement thickness is also an important parameter in general boundary-layer theory; it is defined as the distance through which the wall of a channel carrying a perfect fluid would have to be displaced in order to produce the same reduction in mass flow that is caused by the actual boundary layer.

The diverging portion of an exhaust nozzle is an important feature for all engines which depend upon the thrust produced by exhaust gases. Maximum possible thrust of a nozzle can be obtained by complete expansion of the exhaust gases to the ambient pressure through a nozzle designed to give a parallel uniform jet. One could apply the method suggested by Foelsch (7) for the design of such nozzles. For jet engines operating at high altitudes and especially for rocket motors, one is required to design nozzles for very low ambient pressures. Even the shortest nozzle designed by the aforementioned method would be excessively long and heavy. Logically, one would seek a nozzle of limited length, since length is a fair indication of nozzle weight. The problem then is the choice of a nozzle having a specified length and yielding maximum thrust.

Several methods have been devised for designing optimum thrust nozzles without applying Foelsch's method. One of considerable merit has been introduced by Rao (8). The nozzle length, ambient pressure, and flow conditions in the immediate vicinity of the throat appear as governing conditions under which the thrust on the nozzle is maximized. The first step is to choose a suitable curve for the nozzle wall contour. A circular arc of a multiple of the radius of the throat section is chosen for the nozzle contour upstream of the throat section. (See Figure 17). The line TT' is a constant Mach number line of Mach number greater than unity; therefore, unaffected by downstream conditions. Starting from this line a characteristic flow net can be computed for these initial conditions. Instead of choosing a particular nozzle length, the Mach number, Me, on the nozzle wall at the exit, will be prescribed. This Mach number forms a parameter which describes a posterior the length of the nozzle. By choosing different values for Me, optimum contours for different lengths can be obtained. A nozzle contour obtained for a given length and ambient pressure will also be the contour yielding maximum thrust when the corresponding exit area meets the prescribed conditions.

Isentropic flow is assumed and the variational integral of this maximizing problem is formulated by considering a suitably chosen control surface. The solution of the variational problem yields certain flow properties on the control surface, and the nozzle contour is contructed by the method of characteristics to give this flow.

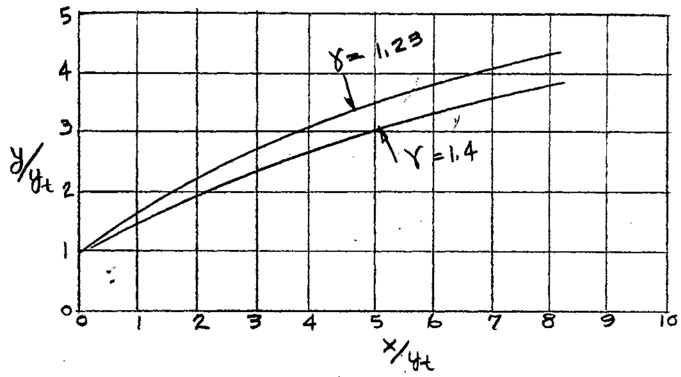

Optimum Nozzle Contours $P_a = 0$

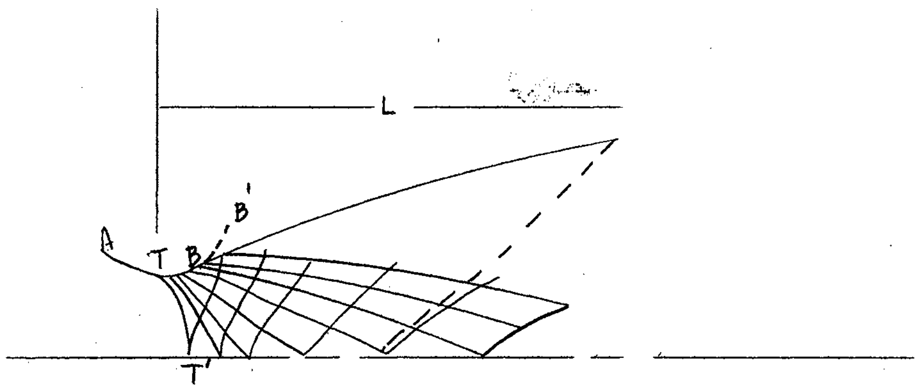

Characteristic Net and Control Surface

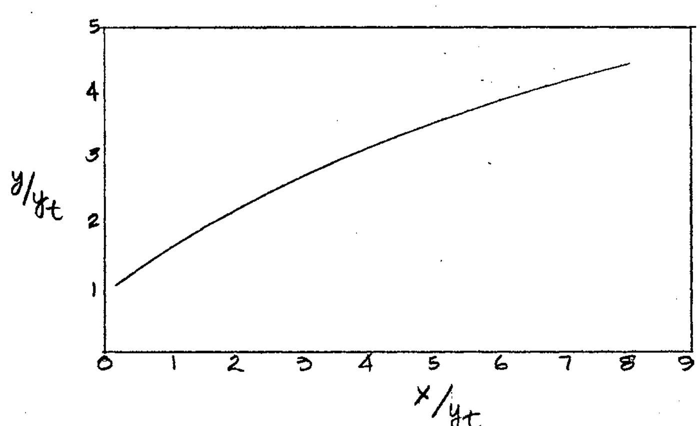

Optimum Nozzle Contours $P_a = 0$ $\gamma = 1.23$

Fig. 17. Optimum Nozzle Contours P_a = ambient pressure

The ratio of specific heats, γ , of the exhaust gases has considerable effect on the optimum contour as can be seen in Figure 17. Comparison of thrust coefficients indicates that the advantage of contoured nozzles is greater at large area ratios.

Another approach has been established by Demuth and Ditore (9). They presented a graphical method for selecting a specific contour and estimating its performance from families of contour and performance curves. The families of contours were developed as streamlines in a transition flow field which joins a source flow with a uniform parallel flow. The method of characteristics for the axially symmetric supersonic flow of a perfect gas was utilized. The performance curves were obtained by integrating pressure and momentum flux over appropriate control surfaces in the flow field. The method of designing a practical nozzle outlined therein entails the choice of a larger expansion ratio nozzle yielding parallel flow at the exit and terminating it at the desired expansion ratio. Using this method, the designer can generate a nozzle shape with a minimum of effort and time, given certain specifications for which the nozzle is intended. It can be shown that this design method when used properly, will yield nozzle shapes very similar to those resulting from the method of Rao, and can be expected to yield nearly the same performance. In general, the nozzle contours and performance curves serve to reduce the complex problems of contouring rocket motor nozzles to the level of reading of charts and subsequent interpolation. The charts and methods are intended to be of use in determining a contour suitable for vehicle system when space, weight, and performance considerations must be made. To obtain the precise performance of the propellant-nozzle combination, corrections to the theoretical values must be made based on tests. Suitable interpretations of and modifications to the procedures indicated must be included to account for grossly nonideal effects such as exist in some of the current rocket exhausts.

From the discussion, it can be seen that the need for experimental research in the area of optimization of thrust nozzles is still great. Along with this, the problems of vector thrust control, plug nozzles, annular nozzles, etc. have become critical areas of development in space craft propulsion systems.

Therefore, the system being designed should have enough flexibility to allow study in all these fields.

CHAPTER V

EJECTOR

The prime purpose for building the thrust nozzle test stand is to study rocket type thrust nozzles. Today most rocket-type nozzles have a $\frac{P_e}{P_o}$ of 15 to 200; we have available a $\frac{P_e}{P_o} = 8$. The simplest and cheapest solution to this seeming mismatch is the use of a self-ejector or "base pressure effect" to lower locally the exhaust back pressure, p, below atmospheric. This ejector method basically consists of an ejector tube situated to encompass the rocket nozzle exhaust jet. As the flow exits, diverging slightly, this jet boundary contacts the ejector wall deflecting in a shock wave. Air is thus entrained in the free jet and, as the shock waves deflect back and forth inside the ejector tube, a diffuser action raises the pressure to atmospheric. As more and more air is thus entrained, a higher vacuum is pulled until some stable pressure ratio is reached. If the ejector tube is correctly designed, realization of the aforementioned pressure decrease can be obtained.

There are a number of elements in the design of such an ejector which should be studied.

1). The ejector assembly and instrumentation should be installed in a manner which will not produce an effect upon the thrust measurement. If this is impractical, it should be possible to calculate any effect the ejector system has upon the actual thrust.

a). There must be a seal in connection with the ejector system. However, if completely sealed by an o-ring of similar device, the thrust will be affected. Therefore, a no-contact seal (labyrinth gland) will be used, realizing that we have introduced leakage. Calculations can be worked out showing a very small resulting effect.

b). The ejector will help create a low pressure on the nozzle base. Corrections for this condition should be made.

2). The nozzle exit flow will leave in a parallel flow with a tendency to bloom out and then buckle in repeatedly. For the ejector to perform its function, proper contact with the jet boundary is critical

a).

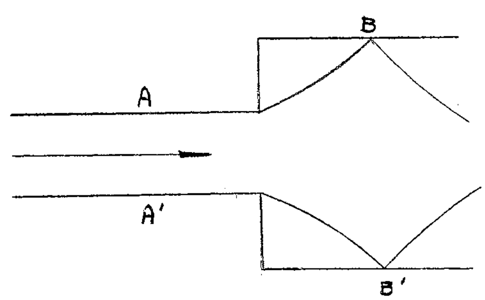

If we should consider an ejector set up such as the one on the left, we would find it necessary to have a variable area ejector tube. The reason for this is that to initially make contact with the flow, the distance BB' would have to be approximately AA'. Upon establishing contact, we would want to increase BB' so as to entrain more air. Thus for physical reasons we reject this approach. A physical setup more easily obtained and perhaps superior is b).

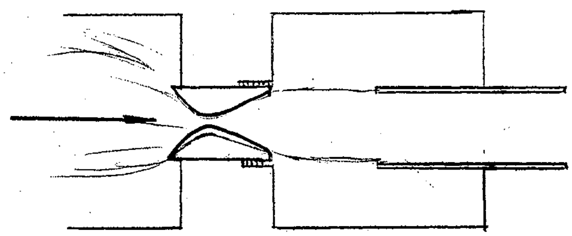

shown on the left. The ejector tube is located so as to just contact the jet boundary. A labyrinth sealed box encompasses the exhaust nozzle exit and part of the ejector tube. Two ports will be situated 180° apart; these are connections for a vacuum chamber system. This system could be used for a very short time to "pull" the jet boundary outward to the ejector tube. We might also incorporate a sliding inner ejector tube sleeve to help make contact with the jet boundary. Once contact is made, the sleeve could be slowly withdrawn, thus changing the equilibrium pressure condition.

3). a). To estimate the leakage through the labyrinth seals, the assumption will be made that our system closely approximates a two-dimensional orifice. A calculation of this leakage will be made.

b). An estimate shall also be made of the leakage effect on the vacuum.

4). From knowledge of the jet boundary for a particular nozzle, we can calculate the ejector size and pressure of the vacuum region.

A theory for ejector performance was developed for a flow model that conformed to experimental results. (13). The model is depicted in Figure 18. The theory requires that the ejector tube be long

Flow Regimes

Case A Flow Separation in Primary Nozzle

Case B Primary Nozzle Flowing Full

Case C Prandtl-Meyer Expansion

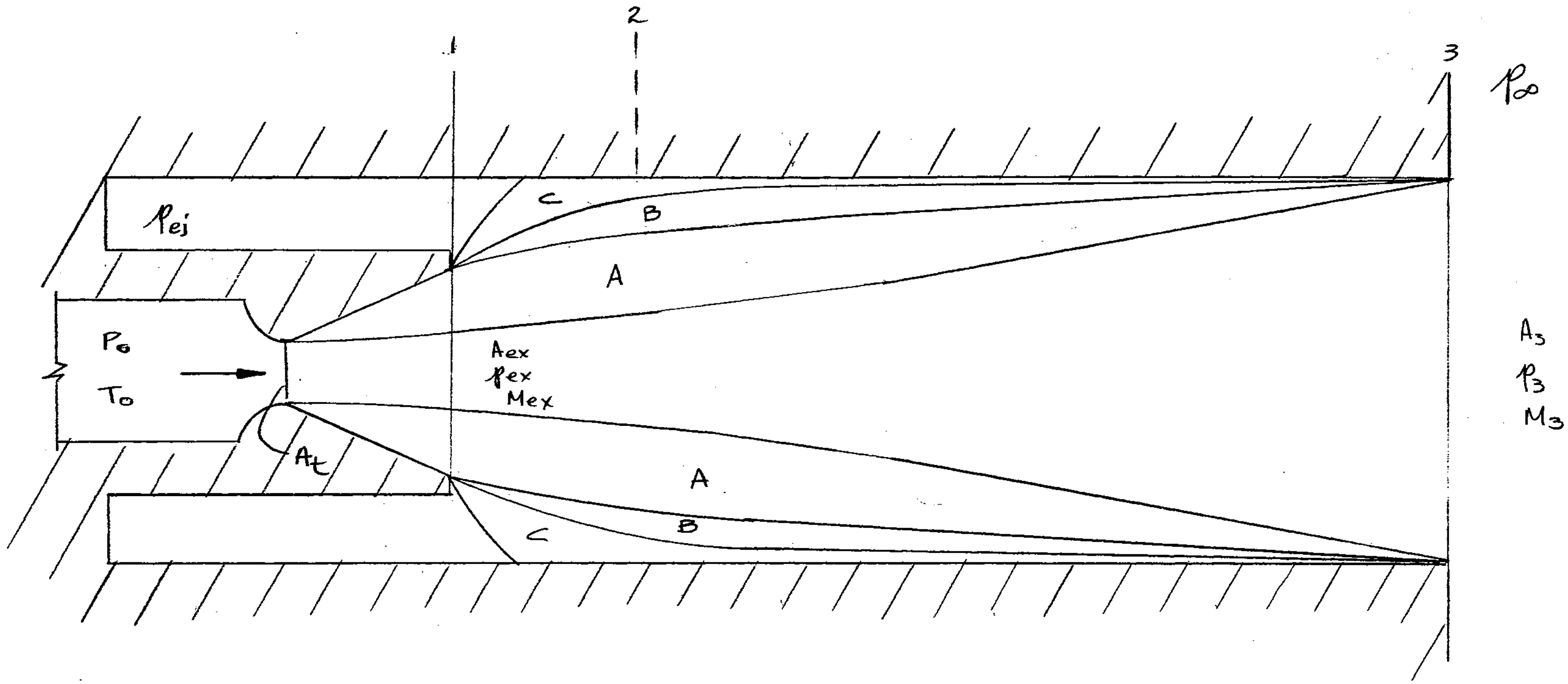

Fig. 18. Ejector Flow Model; No Secondary Flow

enough for its exit to flow full. Assumptions for the theory included one-dimensional, nonviscous, adiabatic flow. A detailed discussion and a comparison of the theory with experimental results is reported in Fortini (13).

From Fortini's work it was found that the pumping fluid leaving the nozzle can evacuate its own environment to an approximate minimum possible value of 0.025 atmosphere. This minimum value appears to be a function of pumping-fluid pressure and ejector-tube area ratio, provided the ejector tube has sufficient length. For ejectors not having sufficient length, the minimum value (different from the optimum) becomes a function of pumping-fluid pressure and ejector length-to-diameter ratio.

Fortini's ejector system experimental apparatus contained a convergent-divergent nozzle with an exit to throat area ratio of 9. A range of ejector-tube area ratios ($\frac{A_3}{A_t}$) from 16 to 49 and ejector-tube length-to-diameter ratios from 2.67 to 12.0 was studied for ratios of pumping pressure to atmospheric pressure. The following results were obtained from a theoretical and experimental investigation of a nonpumping ejector system utilizing cylindrical ejector tubes of various length-to-diameter ratios:

1). The theoretical values obtained by employing the equations of energy, momentum (without fluid friction), and conservation of mass were in good agreement with the corresponding experimental values for long ejector tubes.

2). For large ratios of primary-chamber pressure to ejector-tube back pressure (primary pressure ratio) and for adequate ratios of ejector-tube length to diameter, the expanding primary jet attached to the ejector-tube wall and established shock patterns within the ejector tube. The static pressure of the expanded flow before the initial attached shock wave can be approximated by assuming that it is a function of the ejector-tube to nozzle-throat diameter ratio only.

3). For small primary pressure ratios, the primary nozzle encountered flow separation. The performance of the ejector was affected by flow separation and could be adequately explained by the use of the developed theory, which utilized empirical data for nozzle flow separation.

4). The results indicate a useful means of obtaining a limited range of rocket-engine altitude performance by incorporating the rocket engine as the primary nozzle of an ejector system.

As a method of sealing, we have mentioned labyrinth packing. Leakage past the nozzle-ejector system may be reduced to a small amount by this labyrinth packing where the air pressure is throttled through a succession of very small clearances formed by rings interfitted into the ejector tube. These rings are usually composed of short brass strips with thickness of 0.01 to .015 inches. The number of rings required to limit the leakage of the fluid to a given weight/sec may be determined analytically.

The equation for leakage through an ideal labyrinth (a labyrinth in which the kinetic energy of the fluid jet is completely destroyed and reconverted into heat after each throttling) is similar to the equation for the single throttling. (16).

$$G = A \alpha \phi \sqrt{g \left(\frac{p_o}{v_o}\right)} \qquad (1)$$

where:

G = lb/sec

A = ft^2 (leakage area)

α = Flow coefficient

p_o = lb/ft^2 (absolute pressure before labyrinth)

$\phi = \sqrt{\dfrac{1 - (p_n/p_o)^2}{n + \ln p_o/p_n}}$ (derived for steam but applicable to air and other gases)

p_n = lb/ft^2 (absolute pressure after labyrinth)

v_o = ft^3/lb (sp. volume before labyrinth)

n = number of throttlings

This enables us to predict the leakage through any ideal labyrinth by applying Equation (1) and utilizing Figure 19, once the flow coefficient α has been determined by actual leakage measurements.

$$G = A \alpha \phi \gamma \sqrt{g \left(\frac{p_o}{v_o}\right)} \qquad (2)$$

where

$\gamma = \sqrt{\dfrac{n}{n^1}}$

n = actual

n^1 = strips in equivalent ideal labyrinth

A straight through type labyrinth needs more strips for the same leakage than is required for the ideal labyrinth.

Using Equation (2)

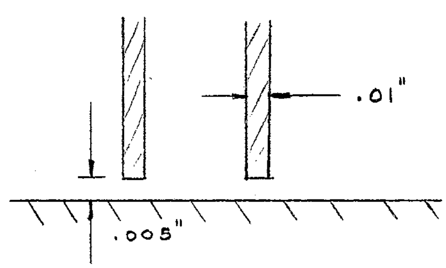

From:

Figure 19 $\phi = 0.29$ for $p_n/p_o = 0.07$

Figure 20 $\alpha = 1.00$ for $\Delta = .01$ and $\delta/\Delta = .5$

Figure 21 $\gamma = 2.00$ for $\delta/s = 100/1000$ and $n = 10$

$p_o = 14.6\ (144)$

$\rho_o = 0.0745$ at 70°F

$A = \pi Dt/144$

$$G = \frac{\pi(2.25)(.005)}{144}[1.0][2.0][.29]\sqrt{32.2(14.6)(.0745)}$$

$$G = (.0295)(.58)(5.95)$$

$$G = 0.0101 \text{ lb/sec}$$

To check the leakage effect as compared with other experimental data by means of a 2-D comparison with a dimensionless bleed number as parameter: (14)

$$\mathcal{H} = \frac{G_B\sqrt{T_o}}{H\ P_o}\sqrt{\frac{R}{g_c K}} \tag{3}$$

where

$R = 53.3\ \dfrac{lb_f\text{-}ft}{lb_m\text{-}°R}$

$g_c = 32.2\ \dfrac{lb_m\text{-}ft}{lb_f\text{-}sec^2}$

$K = 1.4$

$G_B = 0.01$ lb/sec

$T_o = 529$ °R

$H = 1.0$ inch (Geometry)

$$\mathcal{H} = \frac{0.01\sqrt{529}}{1.0(100)}\sqrt{\frac{53.3}{32.2(1.4)}}$$

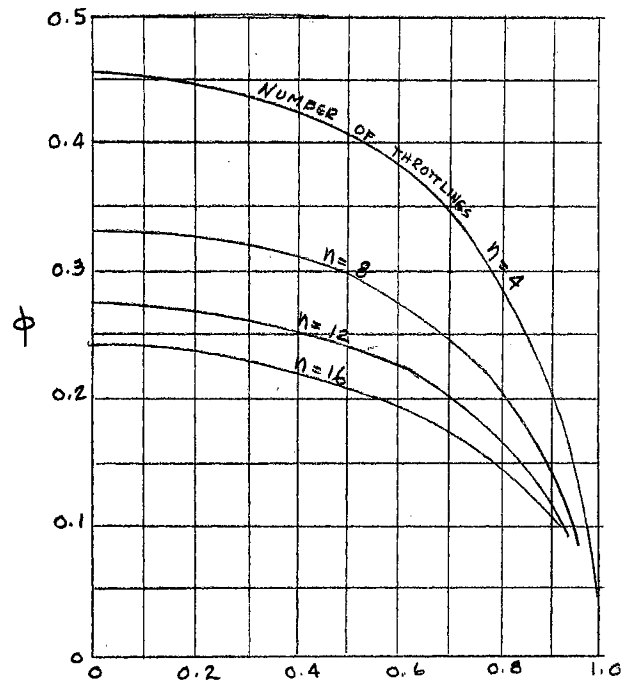

Labyrinth Pressure Ratio p_n/p_o

Leakage Function ϕ for Labyrinths with Four and More Throttlings

Fig. 19. Plot Leakage vs p_n/p_o

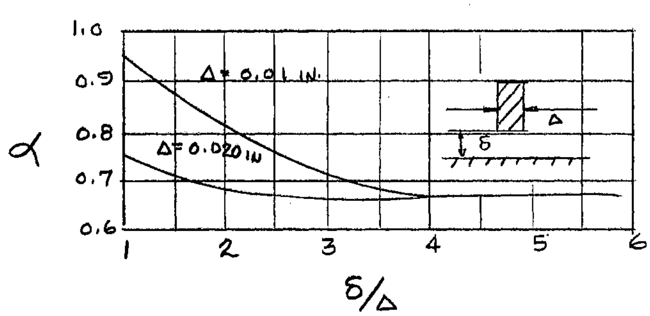

Flow Coefficient α for Labyrinths with Sharp-Edged Strips Determined From Tests

Fig. 20. Plot α vs δ/Δ

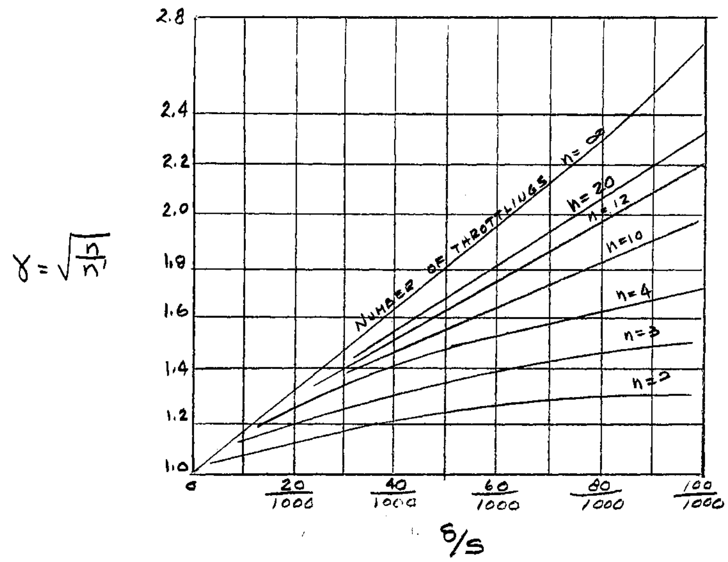

Carry-Over Correction Factor for Straight-Through Labyrinths

Fig. 21. Plot γ vs δ/s

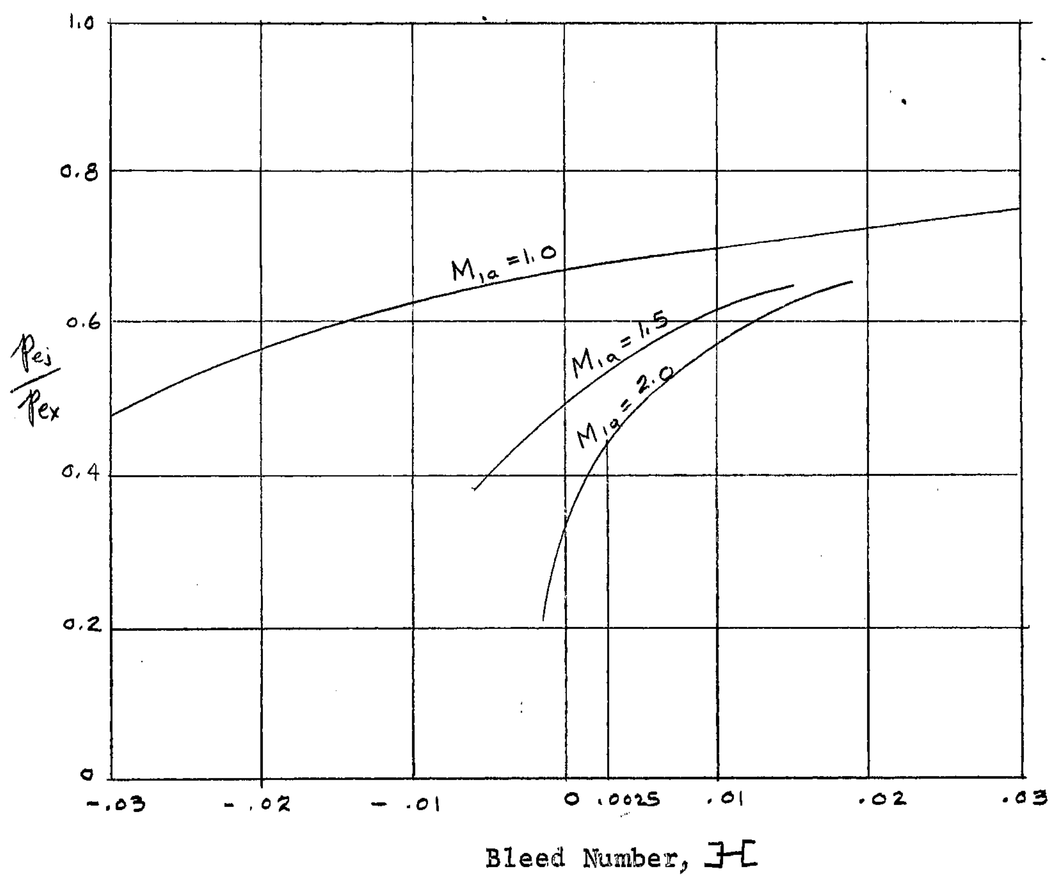

Bleed Number, $\mathcal{H}$

Effect of Bleed Mass (from Ref. 14) on Base Pressure for Two-Dimensional Flow

Fig. 22. Plot p_2/p_1 vs Bleed Number

$$\mathcal{H} = \frac{.01(23)}{100} \quad (1.09)$$

$$\mathcal{H} = 0.0025$$

From Figure 22 (effect of bleed mass)

for $M = 2.0$

$$\mathcal{H} = .0025$$

p_{ej}/p_{ex} changes from 0.35 to 0.425 as a result of bleed. This approximate check shows us that our G_B has little effect upon our pressure.

We can see from TN 392-2 Figure 22 that for our bleed number experimental results show that the leakage we have will not detrimentally affect our ratio of ejector pressure to nozzle exit pressure. One further consideration is that the bleed number was calculated considering a two-dimensional geometry. A look at the geometry of our actual axi-symmetrical condition will show that the two-dimensional geometry yielded a conservative estimate. Therefore, our actual variation will be even less.

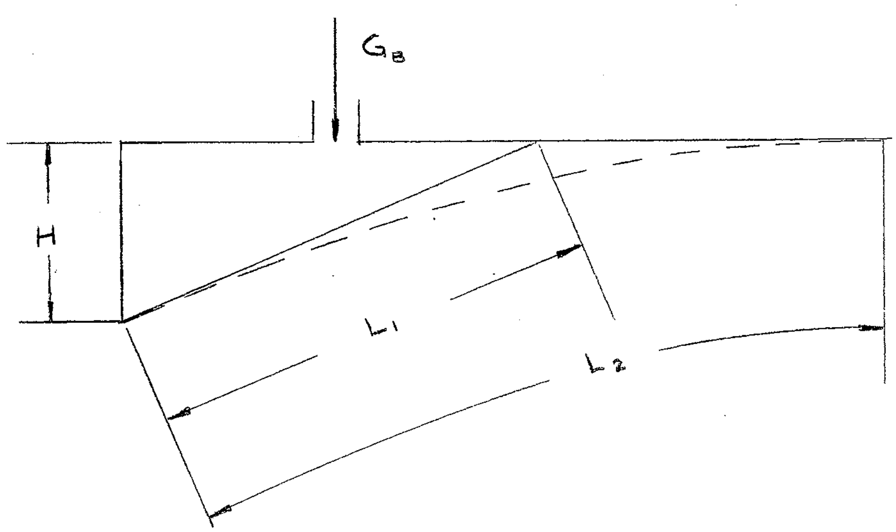

where

L_1 = actual mixing length for 2-D

L = actual mixing length for axi-symmetrical

$\mathcal{H} \sim G_B/L$

if $L_1 < L_2$

G_B = constant

$\mathcal{H}_2 < \mathcal{H}_1$ (thus would diminish the leakage effect)

Consideration should be given to the effect of the base pressure upon the actual thrust of the nozzle. The base pressure will be lower than the nozzle exit pressure and thus it is logical to assume that the base pressure force will be a drag. An analytical approach to the problem should validate our reasoning.

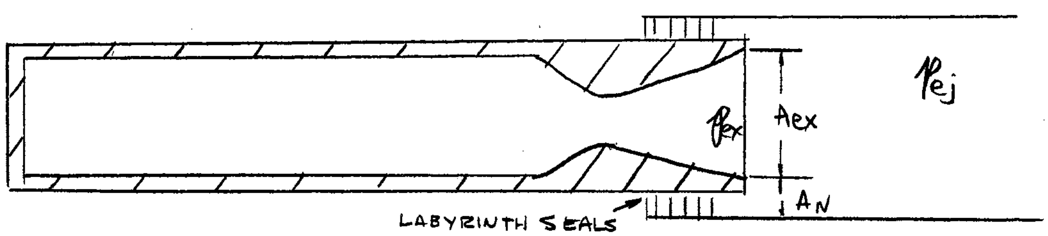

The above figure represents our system.

$$F_c = \rho_{ex} v_{ex}^2 A_{ex} + (p_{ex} - p_{ej}) A_{ex} \tag{4}$$

where

F_c = corrected thrust	ex = exit
A = Area	ej = ejector
v = velocity	F_m = measured thrust
p = static pressure	atm = atmosphere
ρ = density	an = annulus

$$F_m = p_{ex}v^2{}_{ex}A_{ex} + (p_{ex}-p_{atm})\ A_{ex} + (p_{ej}-p_{atm})\ A_{an} \tag{5}$$

Putting Equations (4) and (5) in similar form to determine the correction, if any, necessary to evaluate F_c from F_m:

$$F_m = \rho\ v^2\ A_{ex} + (p_{ex}-p_{ej})\ A_{ex} + (p_{ej}-p_{atm})\ (A_{ex}+A_n)$$

since: $A_{ex} + A_n = A_{total}$

Now combining Equations (4) and (5)

$$F_c = F_m + (p_{atm}-p_{ej})\ A_{total} \tag{6}$$

Base pressure is independent of body length. In supersonic flight, the base pressure is very nearly constant over the base. There is little effect of angle of attack up to about 5^o.

From reference (17), which concerns itself with boundaries of supersonic axi-symmetric free jets exhausting from conically divergent nozzles into still air, a solution to ejector tube size may be calculated. Since 15^o conical divergent nozzles are likely to be used for the thrust stand tests and exhaust is to still air, the reference data should apply. (Figure 23). This NACA report covers jet boundaries for Mach numbers 1.5, 2.0, 2.5, and 3.0 for varying p_{ex}/p_{ej}. The report stated, however, that extrapolations to M_{ej} equal to 3.5 and slightly greater could be obtained with reasonable success. Therefore using the NACA report's curves, plus several extrapolated points (Figure 24), the following were plotted. From these curves a general relationship between the variables, Mach No., y/r_{ex} and x/r_{ex}, was hoped to be obtained. Table I shows the findings.

A check on these conclusions was made possible by Professor

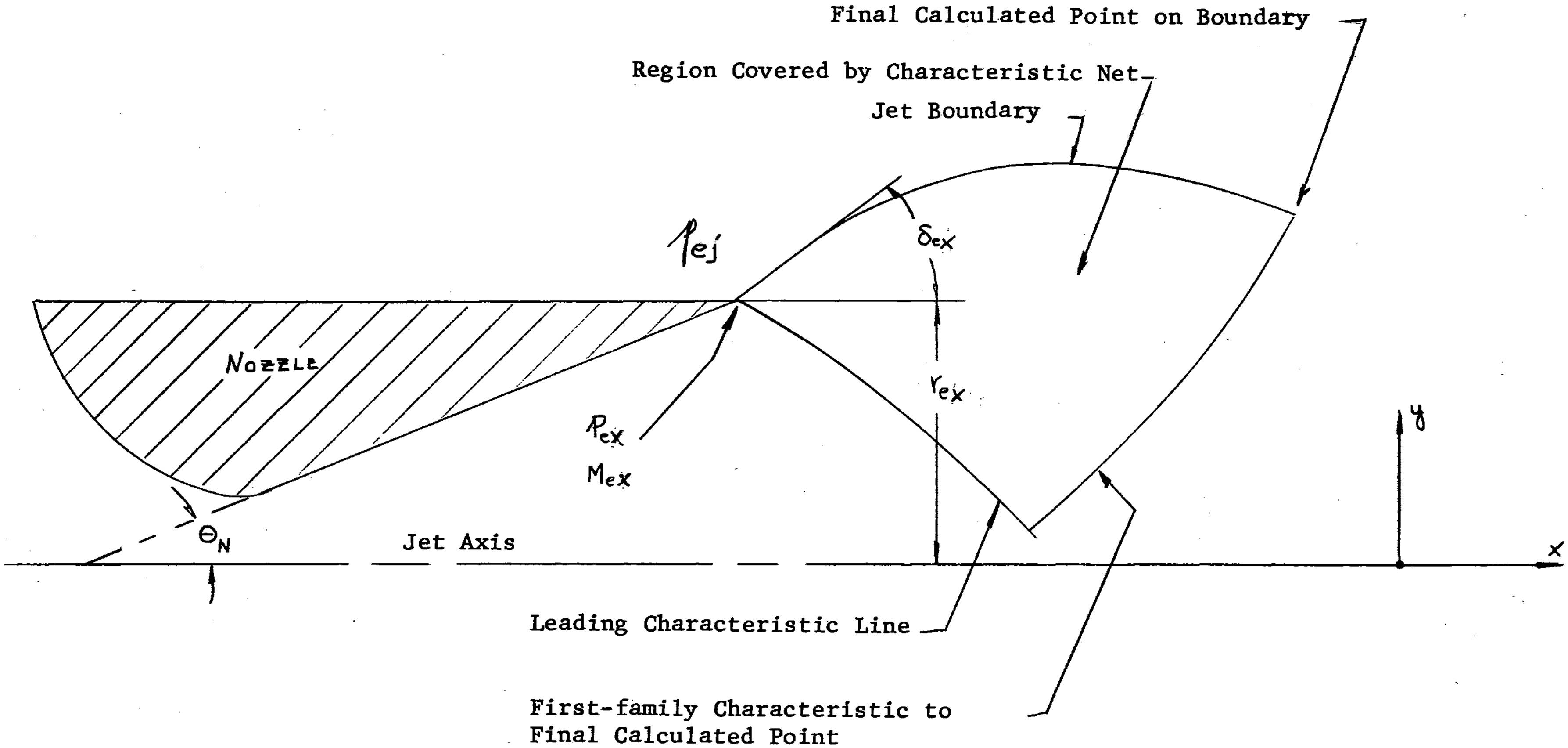

Fig. 23. Sketch of Nozzle, Jet Boundary, and Pertinent Information

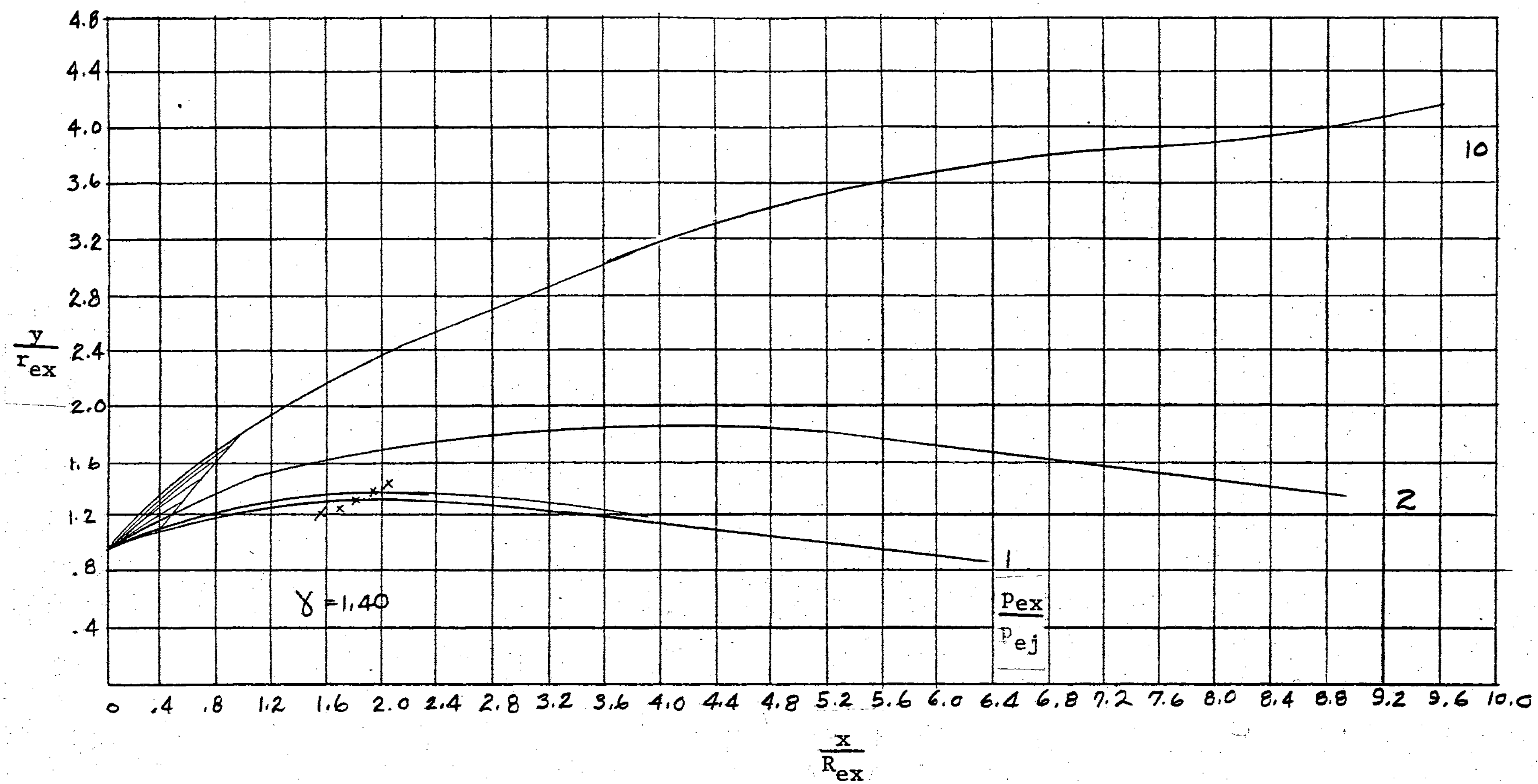

$\theta_n = 15°$

p_{ej} = ejector static

p_∞ = ambient static

r_{ex} = nozzle exit radius

x = distance ⊥ to plane of nozzle exit

y = perpendicular distance from jet axis

Fig. 24. Plot of Jet Boundary on y/r_j and x/r_j Coordinates (NACA)

W. L. Chow, Mechanical Engineering Department, University of Illinois. Dr. Chow had a computer program set up to calculate jet boundaries and he was gracious enough to tabulate some points for the ejector exhaust jet boundary corresponding to given pressure ratios, as shown in Figure 25.

TABLE I

EJECTOR DATA

M_{ex}	$\frac{y}{r_{ex}}$	D_{ej} tube	$\frac{x}{r_{ex}}$	X Variation
2.0	1.21	2.42 r_{ex}	1/2-3/2	1.0 Radii
2.5	1.23	2.46 r_{ex}	1/2-1.8	1.3 Radii
3.0	1.25	2.50 r_{ex}	3/4-2	1.25 Radii
3.5	1.28	2.56 r_{ex}	1-2 1/4	1.25 Radii
3.8	1.30	2.60 r_{ex}	1 1/8-2 1/2	1.375 Radii

The established pattern for the inner diameter of the ejector tube seems to be approximately 2.5 times the radius of the nozzle exit. The variation of length needed shown above is approximately 1.25 radii. The ejector tube will be designed using the largest values in the table for the various parameters. These both occur at the highest M_{ex}. At this Mach number the exit diameter is two inches, making the radius one inch. Since the ejector tube will be mounted as rigidly as possible, a sliding inner-sleeve was designed to allow manual variation in the x (vertical) and y (radial) directions. Radial adjustment is by means of varying thickness sleeves, and vertical adjustment is by raising

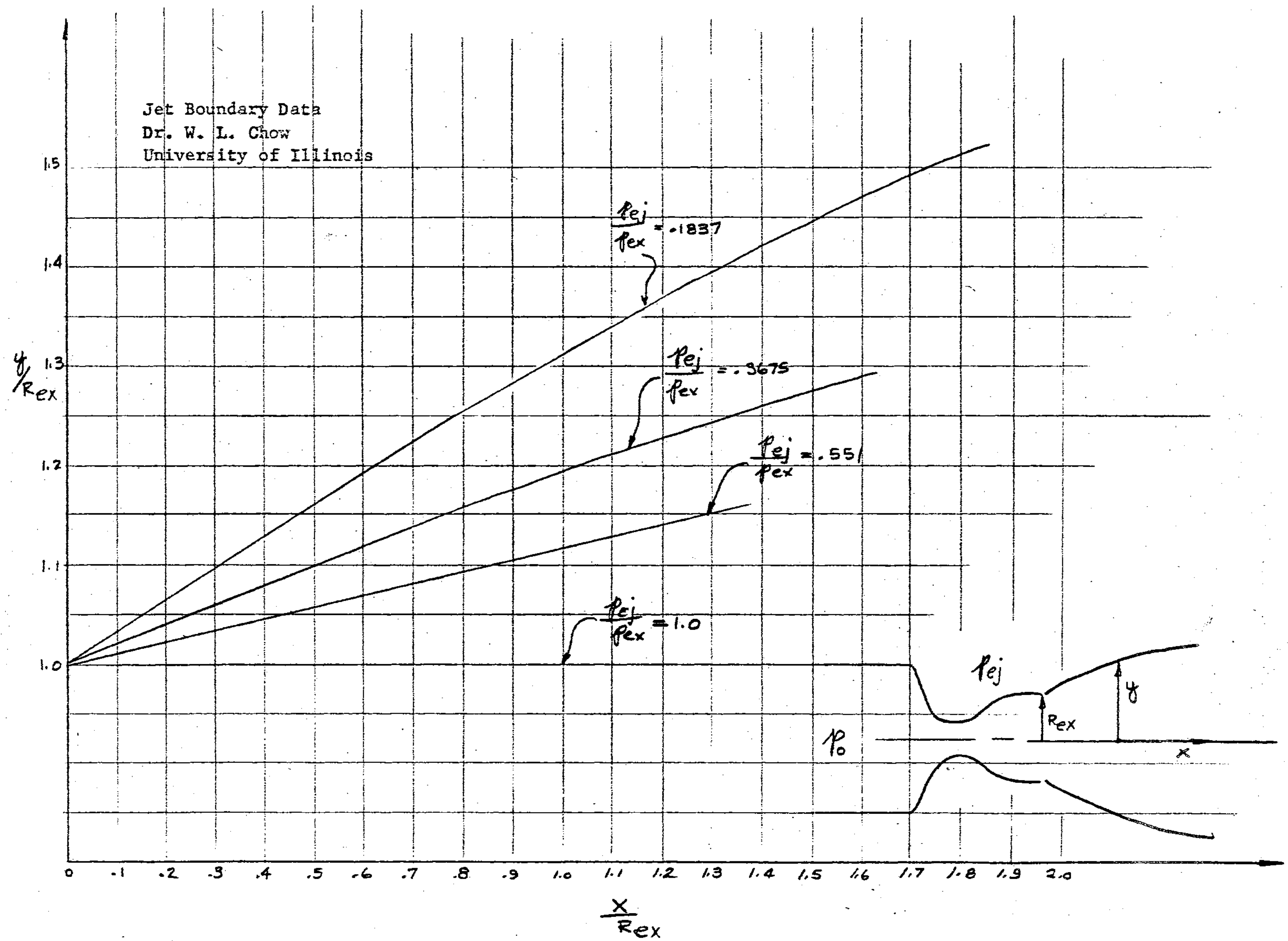

Fig. 25. Jet Boundary Plot

or lowering of the inner sleeve. The assembled drawing of the ejector tube is shown in Figure 26. Two o-rings are inserted in grooved slots to prevent any leakage and also to provide a friction fit for the inner sleeve.

The support and adjustment mechanism for the ejector system is a very real problem. The ejector tube's primary support must be a rigid support to prevent undesirable movements while running the test. The adjusting mechanism must be of such a nature as to provide a fine horizontal adjustment of the ejector plane plus a sliding adjustment in the vertical direction. The critical adjustment is necessary to position the labyrinth seals with minimum clearance but no contact. Figure 27 shows proposed arrangement.

Several calculations concerning ejector tube support shall be made. Assume the weight of the ejector tube acts as a concentrated load. Assume the support acts as a uniformly loaded cantilever beam. Check the bending moment and shear at the support. The ejector outer diameter is 4 inches and has a maximum length of 12 inches.

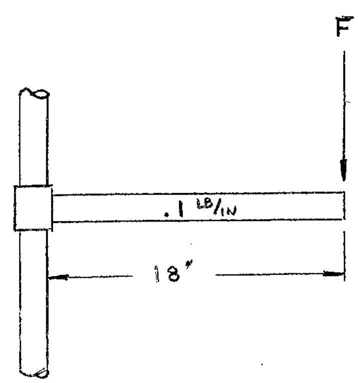

Calculations From Reference (18)

Aluminum = 0.1 lb/in.^{3}

$\text{Volume}_{ej\ tube} + \text{Volume}_{In-sl.} = V_T$

$V_T = 2\pi\ r_{ej}t_{ej}L + 2\pi\ r_{Is}t_{Id}L$

$V_T = 2\pi(2)(\frac{1}{2})12 + 2\pi(3/2)(5/8)(10)$

$V_T = 24\pi + 19\pi$

$V_T = 43\pi$ $\quad F = v \cdot p \quad F = 43\pi(.1) \quad F = 13.5\ lb_f$

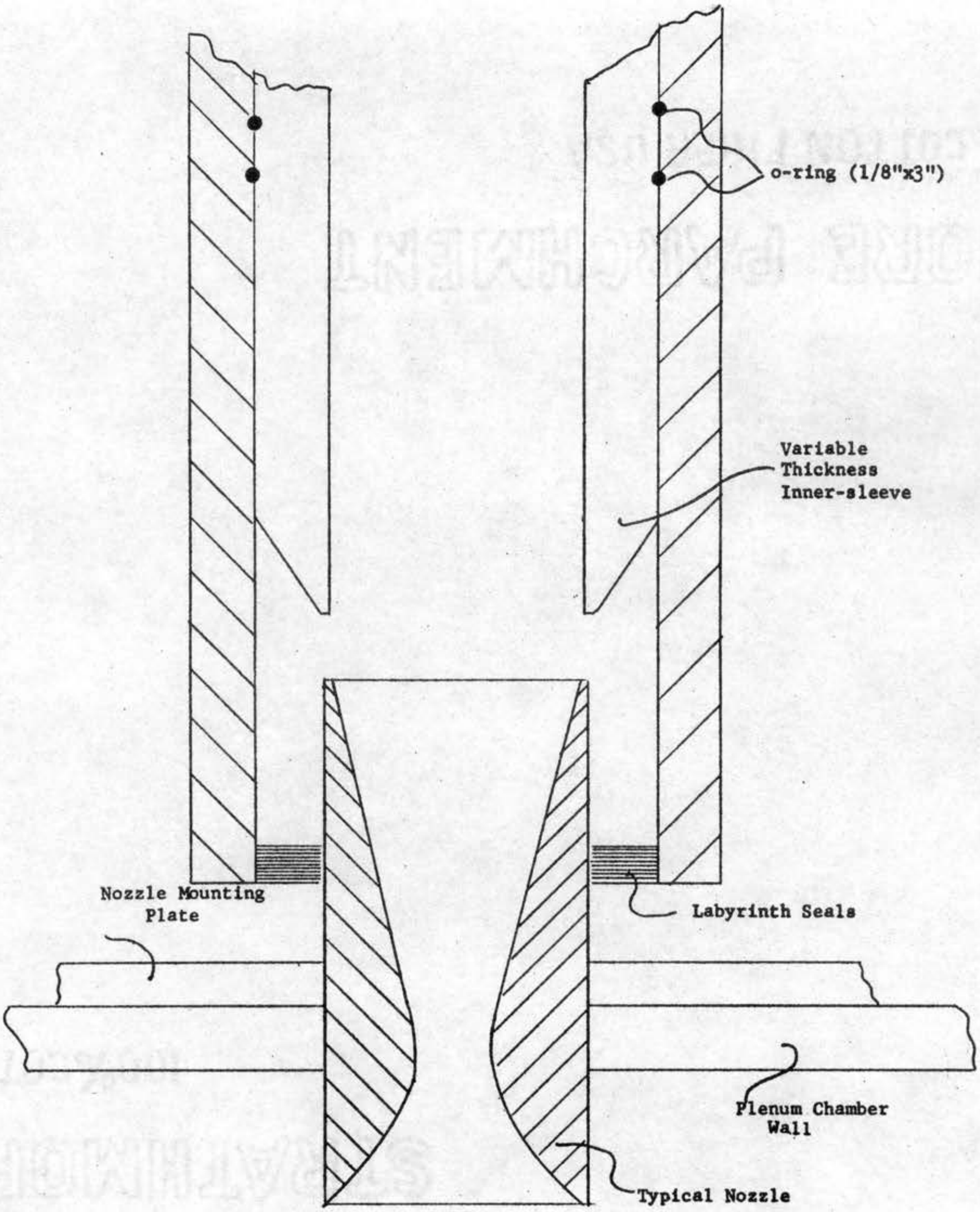

Fig. 26. Scale Drawing of Ejector Tube Assembly

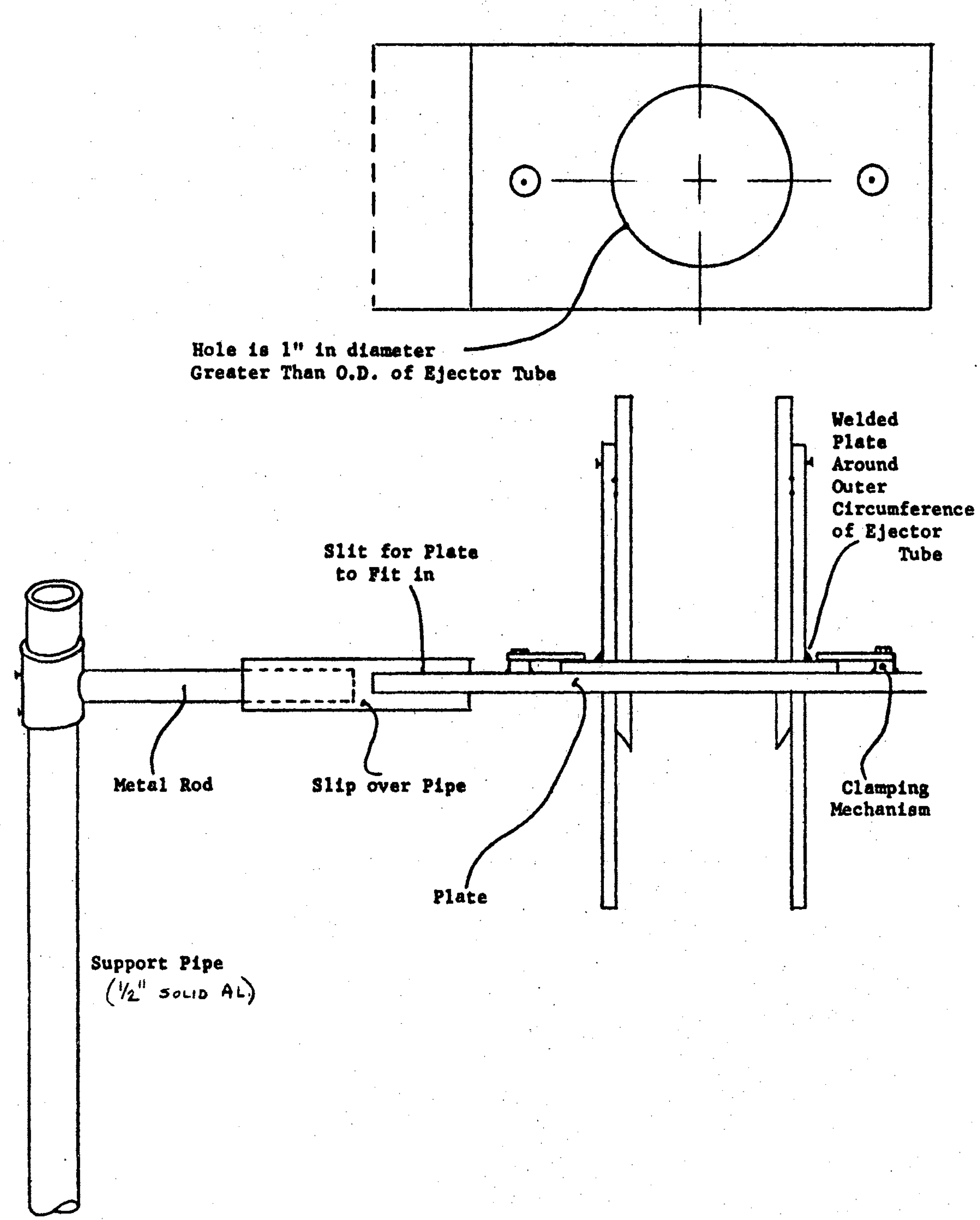

Fig. 27. Ejector Tube Adjustment Method

BENDING MOMENT: $FL = 13.5\ (18)$

SHEAR: $S = F/A$

$$S = 135/\pi/16 = 68.8 \text{ psi}$$

The above calculations indicate a 1/2-inch diameter aluminum rod would have sufficient strength to be used as a support.

The possibility of using a vacuum system to produce the desired effect would normally be financially out of the question. However, the vacuum pump system of the Plasma Jet Generator Project has been made available for use with the thrust stand for future research. The manufacturer's specifications on the vacuum-pump are listed in Appendix E. The incorporation of this into the system will create several new design possibilities, including use of the evacuated tank for initial starting to suck the jet boundaries outward and establish a lower back pressure which will continue after this vacuum surge is expended. This is true because the jet, once attached to the ejector tube, can operate at very low pressures. But the jet will not attach by itself under these same conditions.

CHAPTER VI

THRUST MEASUREMENT

The main objective of this thesis is to design a device capable of measuring the thrust output of various small rocket type nozzles. The rocket nozzles to be used in connection with the test stand will be axi-symmetric nozzles designed for supersonic flow.

The direct measurement of thrust required that the force applied to the measuring instrument be exactly equal to the thrust produced by the rocket or that it be related to the thrust in a definite way. Any other friction or other force which restrains movement of the test stand mount in an unpredictable fashion imposes upon the inherent errors of the measuring instrument additional uncertainty which can not generally be calibrated.

The ideal test stand support would offer no resistance to movement, and this movement itself would introduce no forces extraneous to the thrust which could affect the measurement instrument; consequently the mount could be allowed to move through an indefinite distance to accommodate the instrument. Therefore, some thought and consideration was given to the orientation of the test stand and nozzle arrangement with ease of measurement and method of support being the prime considerations. The decision was made to orient the test stand so that the nozzle exhaust would be directed upward. This particular decision was reached because of space limitations, proposed method of thrust measurement, and facility of working on the test stand.

The test stand, thrust measurement equipment, and location are shown in Figure 28. There are three strain gage thrust pickups, one mounted vertically and the other two mounted horizontally. We shall call the whole thrust pickup unit a flexure load cell system. The load cells were purchased from Aeroscience Inc. of Santa Ana, California and are guaranteed to be linear with force yielding 1/2% over the entire load range. In connection with the load cells Aeroscience Inc. sells flexure pivots which provide movement in three planes about a fixed point in the universal flexure pivot. Financial considerations made it impossible to obtain these flexure pivots. Actually the accuracy that is hoped to be obtained does not require a flexure system of this quality. A flexure system is needed capable of enough flexibility to take any sideward motion that might introduce a torque on the load cell. Any such torque would affect the strain gages and yield a false value for the measured nozzle thrust. A relatively simple but satisfactory flexure joint can be constructed from an ordinary bicycle spoke, two small blocks of metal, and connecting mechanism. A detailed representation of the designed flexure joint is shown in Figure 30. The bicycle spoke was cut into 1¼-inch lengths and mounted in the metal blocks leaving approximately 3/4 inch of free length. The metal blocks are basically 1/2" x 1/2" cylinders with extended 11/32" threaded sections 0.5 inch long. This threaded end screws into the 11/32" threaded hole on the load cell. A 3/32"

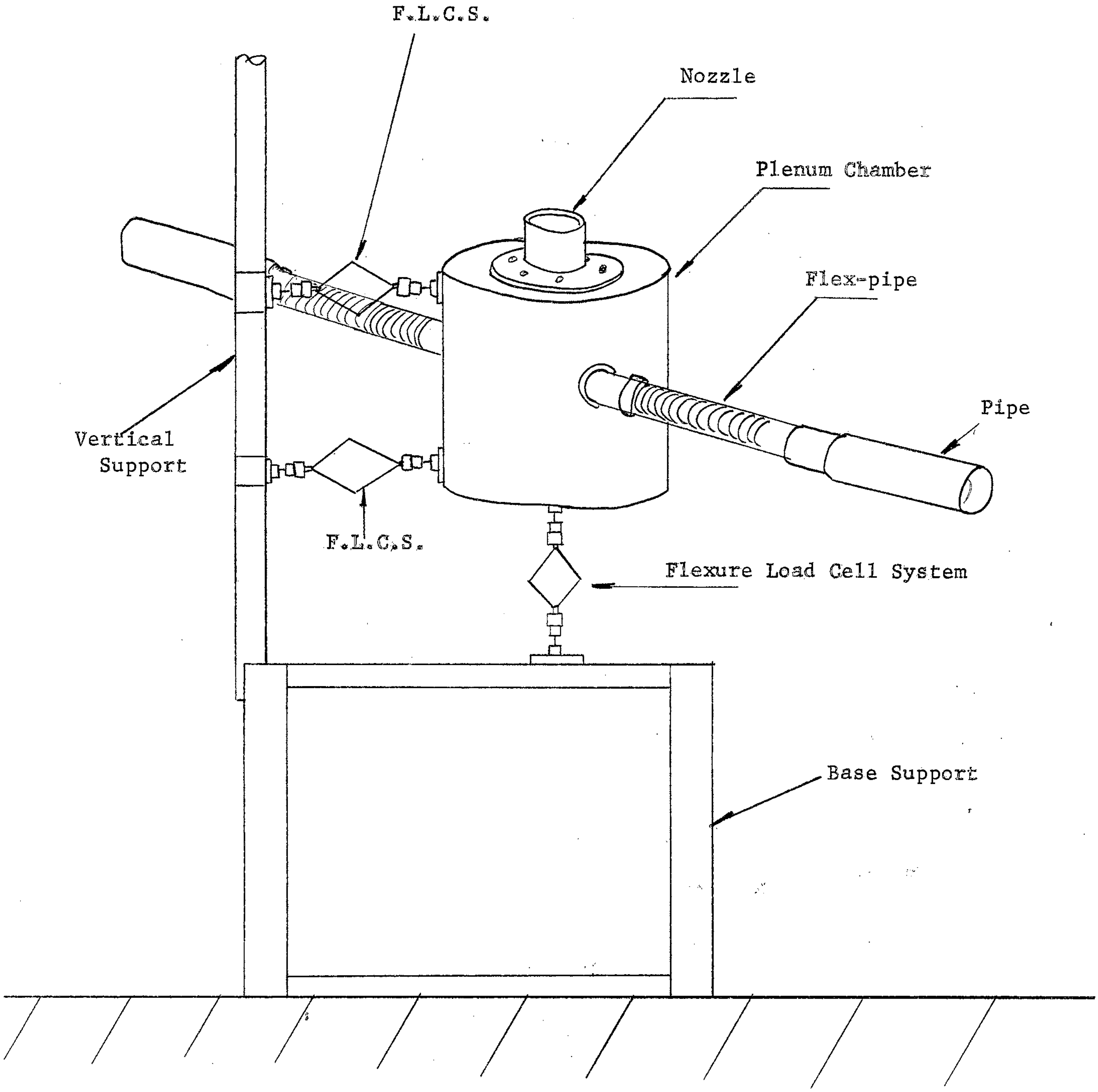

Fig. 28. Flexure Load Cell Systems

diameter key hole must be drilled in each to provide further rigidity. The load cell is approximately 5" x 3" and 3/8" thick. (Figure 29). Three 2" x 2" x 1/2 steel plates were internally threaded with 11/32" centered holes. The other end of the flexure joint was screwed into these plates which had been welded to the plenum chamber in the predetermined locations. The base support was adapted from an existing structure, basically cubical in shape being 24 3/4" (high) x 29" (wide) x 25 1/2" (deep), a welded construction of 2½" x 2½" and 1½" x 1½" angle irons. A three foot 2" diameter 40 gauge pipe was attached in the center of one side 18" from the base. This base support can be attached to the concrete floor if desired.

Instrumentation for the thrust vector measurement requires only a strain-gage bridge-potentiometer. This equipment has not been acquired.

Since the nozzles to be used in conjunction with the test stand are all axi-symmetrical rocket nozzles, the thrust measurement could be obtained by the use of only the vertical flexure load cell system. However, this system was designed with future experimentation and research in mind. Several variations could be introduced in connection with the nozzle. For example, air could be injected downstream of the throat causing the thrust vector to be skewed. By adding one more flexure load cell system in the horizontal system the two components of the thrust vector could be measured. It must be realized, however, that with only these two flexure load cell systems we cannot determine the thrust vector's point of application. The two horizontal flexure

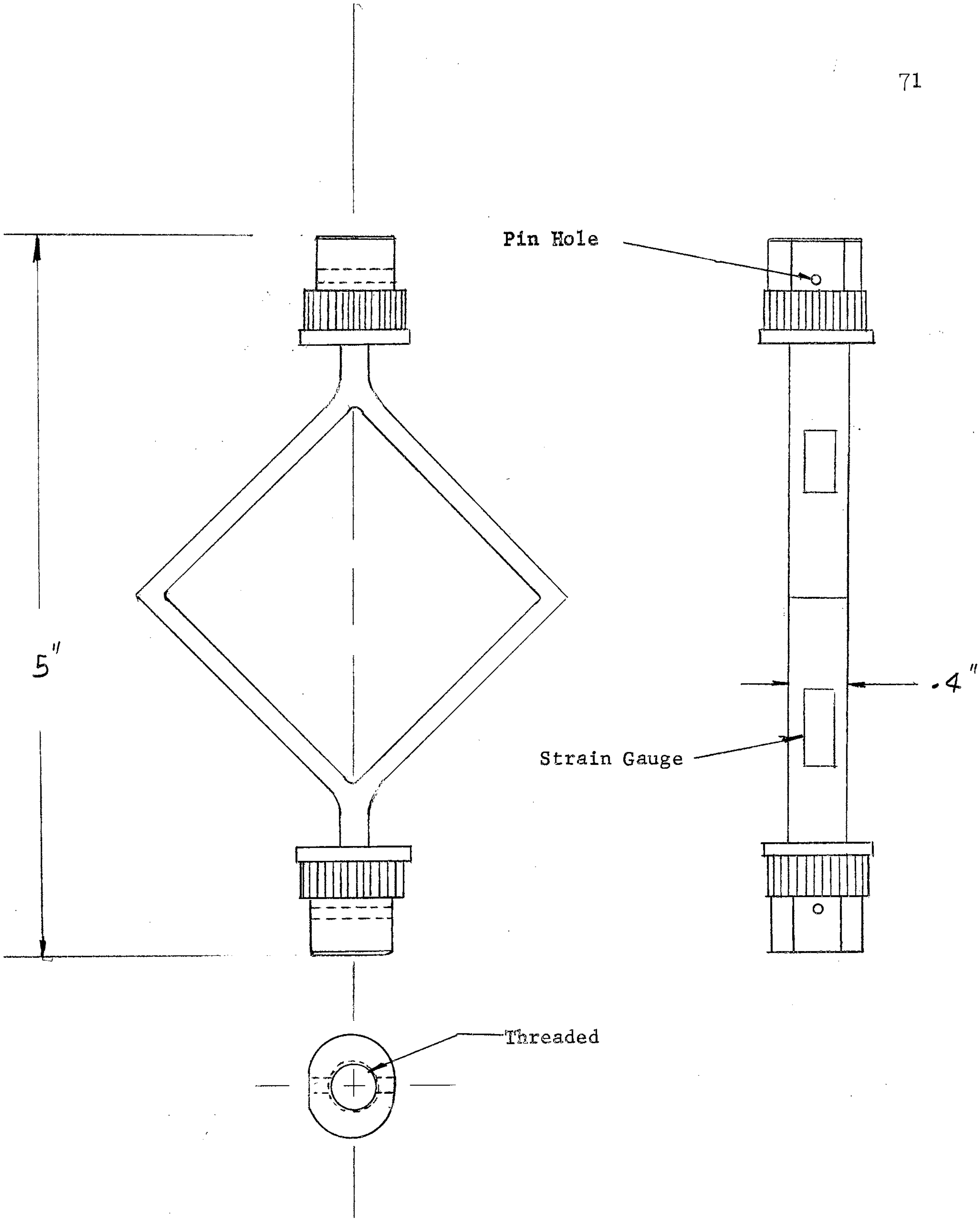

Fig. 29. Flexure Load Cell

load cell systems on this thrust stand design are mounted as far apart vertically as possible while remaining attached to the plenum chamber, as shown in Figure 31. The flexure load system (1) would measure the vertical thrust component while the flexure load cell systems (2) and (3) added together would yield the horizontal thrust component. To locate the thrust vector's point of application, moments can be taken about a point on the nozzle center line in the horizontal plane of flexure load cell system. The thrust vector origin can be defined from these calculations. The actual thrust value will be obtained by taking readings of each load cell strain gage output in millivolts and converting to pounds of thrust by a predetermined conversion.

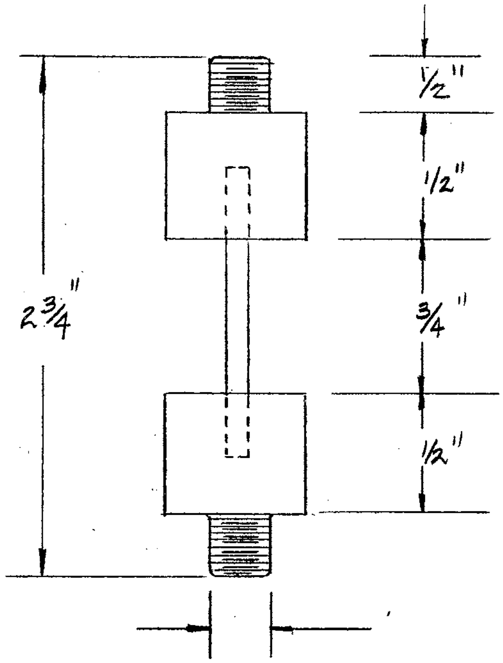

Fig. 30. Flexure Joint

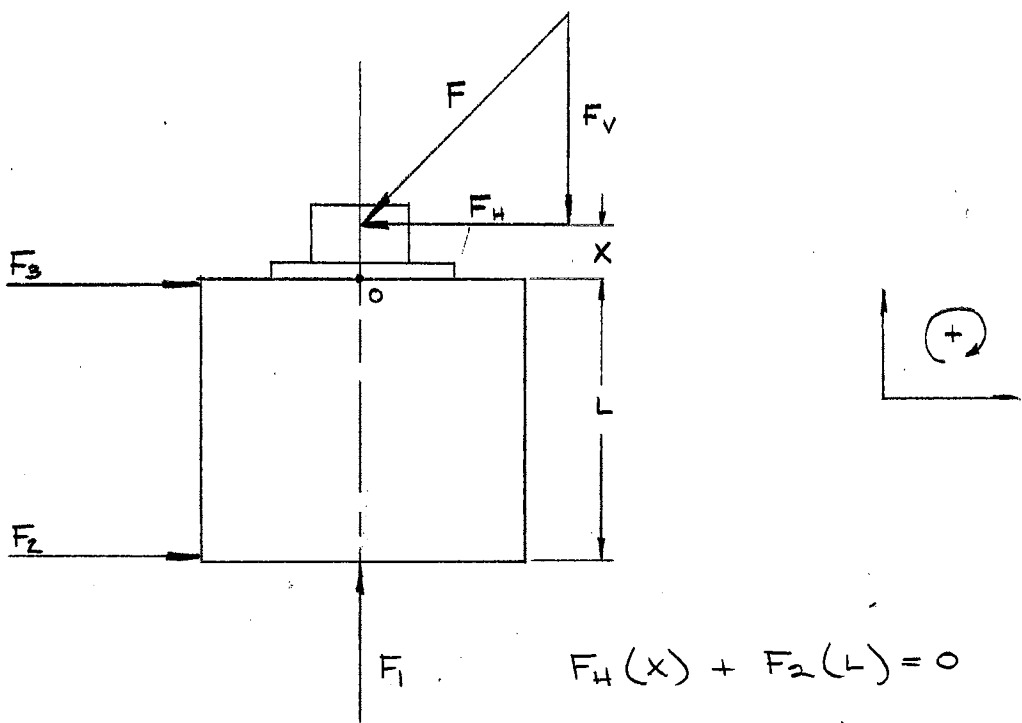

$$F_H = F_2 + F_3$$

$$F_V = F_1$$

$$F_H(X) + F_2(L) = 0$$

$$\therefore \quad X = \frac{F_2(L)}{F_2 + F_3}$$

Fig. 31. Design Thrust Measurement Method

CHAPTER VII

CALIBRATION

The method of calibration technique should be as follows. A reading should be taken with the thrust stand and flexure load cell systems installed, but with no pressure in the system. Then a series of dead weights -- starting with five pounds and increasing in five pound increments until fifty pounds is reached -- should be added to the thrust stand and the load cell output values recorded. From these initial calibrations a relation between millivolt output and pounds of thrust can be determined. This would be a satisfactory method of calibration provided the air pressure in the test stand had no effect upon the load cell readings. To check this possibility, the dead weight series described above should be applied while the plenum chamber is closed and under fifty, and then one hundred, pounds per square inch of pressure. If zero, fifty, and one hundred pounds per square inch of pressure yield the same data as before, then the calibration is independent of pressure. If, however, a variation is found, a method of compensation must be derived.

CHAPTER VIII

FUTURE RECOMMENDATIONS

Although at the time of this writing the thrust nozzle test stand is only in its construction phase and little or no testing has been able to be achieved, it is the writer's belief that the test stand will yield accurate and useful results. Upon final construction and assembly, a calibration program such as outlined earlier will necessarily need to be applied to the thrust nozzle test stand before any valid and exact data can be procured. There are several possible error producing variables whose effect upon the thrust stand measurements should be carefully considered. A very precise measurement of the air reservoir pressure is an essential, initial requirement. Such things as pipe movements, friction in movable joints, leakage of air throughout the entire system, and instrumentation fluctuations are some of the many physical errors that could be detrimental to the overall accuracy of the test stand.

The primary purpose of the test stand is to enable measurement of various rocket nozzles axial thrust output. This should be the first area of future work until the accuracy is established. Future research will be carried out with nozzle variation arrangements. A thrust nozzle with air injected downstream of the throat will produce non-axial thrust forces whose point of application and magnitude should be obtainable. A nozzle using jet flaps and other area variation devices will probably be looked into. A nozzle variation with an aerodynamically controlled throat, possibly by the injection of a regulated amount of air at the throat, should lead to a very interesting and worthy project. Another area of interest might be in the design and testing of nozzle shapes other than conical, such as contoured, plug nozzles, and annular nozzles.

The author also believes that with the combined use of the ejector tube system and the vacuum pump system more extensive research will be possible.

SELECTED BIBLIOGRAPHY

1. Rosenhain, W., "Experiments on Steam Jets," Proceedings I.C.E., Volume 140, 1900, pp. 199-205.

2. Ashwood, P. F., "A Review of the Performance of Exhaust Systems for Gas Turbine Aero Engines," Proceedings I. Mech. E., Volume 171, 1956, p. 129.

3. Rowe, R. N., "Laboratory Methods of Measuring Thrust," Imperial College Report J. R. L., No. 37, 1957, Ministry of Supply, England.

4. Sibley, F. H., and T. S. Kemble, "Efficiency of Steam Turbine Nozzles," Transactions A.S.M.E., Volume 31, 1909, p. 1169.

5. Fraser, R. P., Rowe, P. N., and M. O. Coulter, "The Efficiency of Supersonic Nozzles for Rockets and Some Unusual Designs," Proceedings I. Mech., Volume 171, p. 553.

6. Stanton, T. E., "On the Flow of Gases at High Speeds," Proceedings Royal Society, Volume 111a, 1926, p. 306.

7. Foelsch, K., "The Design of an Axially Symmetric Laval Nozzle for a Parallel and Uniform Jet," Journal of the Aeronautical Sciences, March, 1949.

8. Rao, G. V. R., "Exhaust Nozzle Contour for Optimum Thrust," Jet Propulsion, 28, June, 1958, pp. 377-82.

9. Demuth, O. J., and M. J. Ditore, "Graphical Methods for Selection of Nozzle Contours," American Rocket Society, January, 1960, pp. 1045-60.

10. Winer, Richard and L. Morey, "Nozzle Design for Solid Propellant Rockets," American Rocket Society, January, 1960, 1046-60.

11. Overall, Robert E., " An Experimental Comparison of Contoured and Conical Nozzles," American Rocket Society, 1044-60.

12. Dillaway, Robert B., "A Philosophy for Improved Rocket Nozzle Design," Jet Propulsion, Volume 27, n. 10, pp. 1088-1093.

13. Fortini, Anthony, "Performance Investigation of a Non-Pumping Rocket-Ejector System for Altitude Simulation," NASA, TN D-257, 1959.

14. Korst, H. H., "A Theory for Base Pressures in Transonic and Supersonic Flow," M.E. Technical Note 392-2, U. of Illinois, Urbana, Illinois.

15. Committee, "Rules for Construction of Unfired Pressure Vessels," Section 8, A.S.M.E. Boiler Construction Code, A.S.M.E., New York, 1956.

16. Egli, A., "Leakage of Steam Through Labyrinth Seals," A.S.M.E. Transactions, Volume 57, April, 1935, pp. 115-22.

17. Love, Eugene S., and M. J. Woodling, "Boundaries of Supersonic Axisymmetric Free Jets," NACA, RML56G18, 1956.

18. Marks, Lionel S., "Mechanical Engineers Handbook," McGraw-Hill Book Co., Inc., New York, 1951, p. 940 and 1157 (General).

19. Foelsch, Kuno, "A New Method of Designing Two-Dimensional Laval Nozzles for a Parallel and Uniform Jet," North American, Report 46-235-2, 1946.

20. Bierlein, J. A. and Scheller, K., "Methods of Measuring Thrust," Journal of American Rocket Society, Vol. 23, 1953, p. 128.

21. Durham, Franklin P., "The Performance Characteristics of Small Rocket-Type Nozzles," Report 6, N-123S-82337, T. O. 1, University of Colorado, 1955.

APPENDIX A

MACHINERY ROOM EQUIPMENT DATA

a. Engine:

Make: Hercules Motor Co.

Model: HXD

H. P.: 250 BHP (max)

Size: 5½" (bore) x 6" (stroke)

Cylinder: 6

Ignition: Dual

Cooled: Water

Fuel: Natural Gas

Transmission: White Motor Co.

b. Compressor:

Make: Balcke Machinenbau

Model: 1944

Type: Rotary Vane

Compression Ratio: 8:1

CFM: 800

Max. Temp: 300°F

Lubricant: Cellube (Synthetic Oil)

Two Stage

c. <u>Aftercooler</u>:

Make: Western Supply Co.

Model: C-908-G

Constr.: All welded (API-ASME)

Size: 2' dia x 13'

Tubes: 124 - 3/4" O.D. - 16 Ga. Welded Steel Tubes 10' long

Heads: Floating and cover

Passes: 4

d. <u>Air Receiver</u>:

Make: Black, Sivalls and Bryson, Inc.

Model: S30-10

Size: 30" O. D. x 8'0"

Working Pressure: 160 psi

Flanges: Inlet and outlet

e. <u>Dryer</u>:

Make: National Tank Co.

Model: -2947

Size: 24" O. D. x 10'-0" shell

Working Pressure: 125 psi at 100°F

Material: ASTM

Dessicant: Mobil sovabead

f. <u>Heater</u> (Regenerator)

Make: O.S.U. Temp. Control

Model: Natural Gas Forced Convection

Fan: 13 in. H_2O Head

Output: 30,000 BTU at 50 C.F.M.

APPENDIX B

FLOW METERING NOZZLE

General Conditions

Flow: 0.5 lb/sec to 1 lb/sec

Temperature: 540°R

Pressure: 100 psi

Pipe Size: 3 inch nominal

Design according to ASME Power Test Code 1949
Chapter 4 "Flow Measurement"

From Section 5 of Chapter 4

$$w = \frac{YKE}{12} A_2 \sqrt{2 g p \Delta \rho} \tag{1}$$

$$A_2 = \frac{12w}{YKE \sqrt{2 g p \Delta \rho}} \tag{2}$$

$$D_2 = 2 \sqrt{\frac{A_2}{\pi}} \tag{3}$$

Specific Volume:

$$V = \frac{RT}{P} = \frac{53.35(540)}{14.7 (144)} = 1.745 \text{ ft}^3/\text{lb}$$

Minimum Pressure Drop:

$$\Delta P = 7(.0360 \text{ lb})(12.55) = 3.2 \text{ psi}$$

Calculation of Primary Area (Eqn. 2)

$$A_2 = \frac{(1)(.5)}{YKE (.668) \sqrt{\Delta p/\rho}}$$

Estimate YKE = 1.0

$$\therefore A_2 = \frac{.5}{1.0\,(.688)(1.352)}$$

$$A_2 = .530 \text{ in}^2$$

Throat Diameter: (Eqn. 3)

$$D_2 = 2\sqrt{\frac{.530}{\pi}}$$

$$D_2 = 0.8393 \text{ in.}$$

Diameter Ratio:

$$D_2/D_1 = \frac{.8393}{3.0} = 0.280$$

Area Ratio:

$$(D_2/D_1)^2 = (.280)^2 = 0.0783$$

Reynolds No.:

$$R_e = \frac{48(.5)(12)}{\pi(3)(3.9\text{x}10^{-7})} = 7.82 \text{ x } 10^7$$

Flow Coefficient:

$$K = 1.058$$

Ø from Table (6):

$$\emptyset = 0.993$$

Thermal Expansion Factor:

$$E = 1.0$$

Actual YKE:

$$YKE = 1.0(1.058)(.993) = 1.05$$

$$P_{max} \cong \left(\frac{w_{max}}{w_{min}}\right)^2 \Delta P$$

$$P_{max} \cong \left(\frac{1.0}{.5}\right)^2 (7.15) = 28.60 \text{ in } H_2O$$

Flow metering nozzle dimensions are found on page 26 in code. Plot for use in connection with this nozzle is coefficient of discharge vs. Reynolds Number and is a function of A_2/A_1. (Figure 18, p-26 Code)

APPENDIX C

PLENUM CHAMBER DESIGN

Calculation of Wall Thickness (In accordance with ASME Code)

a. Application

[U-1] $(P-15)(D-4) > 60$

$(P-15)(V-1.5) > 22.5$

Plenum Chamber Conditions

$P_{max} = 130$ psi

$D = 12$ in.

Vol. $= \pi/4$ ft^3

$(130-15)(12-4) = 920 > 60$

$(130-15)(.78-1.5) = 80.5 > 22.5$

[U-20] Shells for Internal Pressure

$$t = \frac{PR}{SE-0.6P}$$

s = stress from Table U-2 (psi)

t = thickness (inches)

E = efficiency of weld

R = radius (inches)

Seamless Pipe: E = 1.0

Radius = 6.0"

Stress = 9000

$$t = \frac{130(6)}{9000-0.6(130)}$$

t = 0.1 inch (use 40 gauge pipe)

[U-39] Flat Heads

$$t = d\sqrt{\frac{CP}{S}}$$

where: t = minimum thickness (inches)

d = diameter (inches)

S = Maximum allowable working stress (psi)

C = coefficient of attachment

C = 0.25 for heads forged integral with or butt welded to vessel

α = 12.0 inches

P = 130 psi

S = 12,000 psi

$$t = 12\sqrt{\frac{.25(13\cancel{0})}{12,00\cancel{0}}}$$

$$t = 12\sqrt{.00271}$$

$$t = 12(.052)$$

t = .624 inch [use 5/8"]

[U-59] Nozzle Openings

a. Fig. U-8 with $K < 25\%$

2" opening does not need reinforcing

[U-64] Hydrostatic Test

P = 195 psi P = 1.5 Pu

[U-76] Stress Relieving

All fusion-welded vessels. Air pipe is seamless.

Calculation of Weld Strength [Welding qualifications Sec. 9]

$$\text{Area} = \frac{\pi D^2}{4} = \frac{144\pi}{4}$$

$$= 113 \text{ in}^2$$

$$\text{Force} = PA$$

$$= 100 \text{ psi } (113 \text{ in}^2)$$

$$\text{Force} = 11{,}300 \text{ lb}_f$$

Weld Thickness

$$S = \frac{F}{Ct}$$

$$S = \frac{11{,}300}{12\pi(\frac{1}{4})}$$

$$S = 1200 \text{ psi} \quad [\text{O.K.}]$$

S = stress

F = force

C = Circumference

t = leg height

Weld will carry 3000 psi in dynamic shear

APPENDIX D

NOZZLE DESIGN CALCULATIONS

Available Conditions

a. Compressor: 800 ft^3/min, p = 14.7, T = 550°R

b. Nozzle: P_o = 110 psia, T_o = 550°R, P* = 58.1 (110 (.528)
critical M = 1

Solving for maximum Mach number with normal shock located at exit (slightly outside)

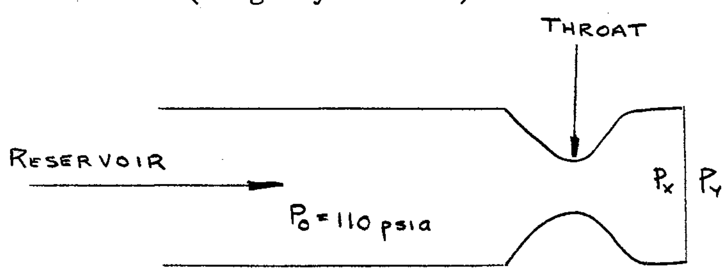

Using the weight flow function considering Mach = 1 exits at the throat.

$$\frac{\dot{W}\sqrt{T_o}}{A^* \ P^*} = 1.0070 \qquad [\gamma = 1.4)$$

$$W = \frac{PV}{RT} = \frac{14.7(144)(\frac{800}{60})}{53.3\ (550)} = 0.968 \text{ lb/sec}$$

For design reliability assume the compressor delivers 0.850 lb/sec.

$$\therefore A^* = \frac{.850\ \sqrt{550}}{58.1(1.007)} = 0.341 \text{ in}^2$$

Calculate the Throat Diameter

$$D_t^2 = 4/\pi(.341)$$

$$D_t = 0.658 \text{ in.}$$

Maximum Mach Number

$$Py = P_o \frac{Px}{Po} \frac{Py}{Px}$$

For $M = 3.85$ [From NACA report 1135]

$$Py = 110(.0806)(17.13)$$

$$Py = 15.2 \text{ psia}$$

$Py > P_b$ $\therefore$ Shock stands slightly outside nozzle exit.

Exit Diameter

For $M = 3.85$ From NACA (Report 1135)

$$\frac{A^*}{A_{exit}} = \frac{1}{9.366}$$

$$A_{exit} = \frac{.341}{.1070} = 3.185 \text{ in}^2$$

$$D_e^2 = 4/\pi(3.185 \text{ in}^2)$$

$$D_e = 2.015 \text{ in.}$$

APPENDIX E

Kinney high vacuum pump [Model KDH-220]

Single stage - Duplex design

Ultimate design 10 microns - McLead gauge

Free Air Displacement - 218 cfm

RPM - 415

Motor HP - 10

Motor RPM - 1800

Oil Capacity - 13 gal.

Cooling - 2.33 gpm at 60°F (H_2O)

Shaft Dia. - 1-5/8"

Inlet Connection - 6" Flange

Outlet Connection - 3" Screwed

Valve Type - Deck Poppet

Separator Tank - Kinneyswirl

Net Weight, Complete Unit - 2100 lb

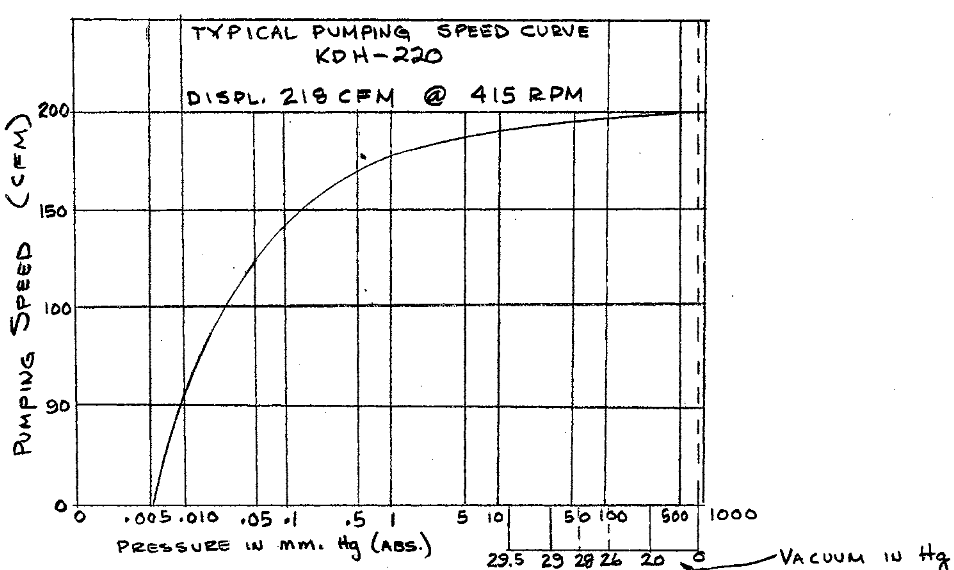

Pumping Speed Curve

VITA

Gerald Robert Seemann

Candidate for the Degree of

Master of Science

Thesis: DESIGN OF AN EXPERIMENTAL THRUST NOZZLE TEST STAND

Major Field: Mechanical Engineering

Biographical:

Personal Data: Born in Melrose Park, Illinois, March 29, 1937, the son of Robert W. and Leona K. Seemann.

Education: Graduated from Polytechnic High School, Fort Worth, Texas, June, 1955; entered Texas Technological College in September, 1955, and received the Bachelor of Science degree in Mechanical Engineering in June, 1959. Entered Oklahoma State University in September, 1959; completed the requirements for Master of Science degree in Mechanical Engineering, August, 1960.

Experience: Worked one summer for Hedrick and Stanley, Architects and Engineers, Fort Worth, Texas, and two summers for Chance Vought Aircraft Co., Grand Prairie, Texas.

Professional Organizations: The writer is a member of the following: The American Society of Mechanical Engineers, The American Rocket Society, Phi Eta Sigma, Kappa Mu Epsilon, Tau Beta Pi, Phi Kappa Phi, and Pi Tau Sigma.